Table 1 List of host proteins interacting with HCV Core and NS4B proteins, identified by Y2H screens

List of host proteins interacting with the Core protein		
Gene ID	Official symbol	Description
1937	EEF1G	Eukaryotic translation elongation factor 1 gamma
1964	EIF1AX	Eukaryotic translation initiation factor 1A, X-linked
2023	ENO1	Enolase 1 (alpha)
2109	EFTB	Electron-transfer-flavoprotein, beta polypeptide
2512	FTL	Ferritin, light polypeptide
292	SLC25A5	Solute carrier family 25 (mitochondrial carrier; adenine nucleotide translocator), member 5
4720	NDUFS2	NADH dehydrogenase (ubiquinone) Fe–S protein 2, 49 kDa (NADH-coenzyme Q reductase)
5265	SERPINA1	Serpin peptidase inhibitor, clade A (alpha-1 antiproteinase, antitrypsin), member 1
5688	PSMA7	Proteasome (prosome, macropain) subunit, alpha type, 7
81502	HM13	Histocompatibility (minor) 13
9804	TOMM20	Translocase of outer mitochondrial membrane 20 homolog (yeast)

List of host proteins interacting with the HCV NS4B protein		
Gene ID	Official symbol	Description
10130	PDIA6	Protein disulfide isomerase family A, member 6
10682	EBP	Emopamil binding protein (sterol isomerase)
116844	LRG1	Leucine-rich alpha-2-glycoprotein 1
1209	CLPTM1	Cleft lip and palate associated transmembrane protein 1
132299	OCIAD2	OCIA domain containing 2
1528	CYB5A	Cytochrome b5 type A (microsomal)
154467	C6orf129	Chromosome 6 open reading frame 129
1571	CYP2E1	Cytochrome P450, family 2, subfamily E, polypeptide 1
196410	METTL7B	Methyltransferase like 7B
200185	KRTCAP2	Keratinocyte associated protein 2
2013	EMP2	Epithelial membrane protein 2
2147	F2	Coagulation factor II (thrombin)
2220	FCN2	Ficolin (collagen/fibrinogen domain containing lectin) 2 (hucolin)
2266	FGG	Fibrinogen gamma chain
2267	FGL1	Fibrinogen-like 1
27173	SLC39A1	Solute carrier family 39 (zinc transporter), member 1
2731	GLDC	Glycine dehydrogenase (decarboxylating)
286451	YIPF6	Yip1 domain family, member 6
334	APLP2	Amyloid beta (A4) precursor-like protein 2
335	APOA1	Apolipoprotein A-I
338	APOB	Apolipoprotein B (including Ag(x) antigen)
3732	CD82	CD82 molecule
4267	CD99	CD99 molecule
4513	COX2	Cytochrome c oxidase subunit II
4538	ND4	NADH dehydrogenase, subunit 4 (complex I)
4924	NUCB1	Nucleobindin 1
51075	TMX2	Thioredoxin-related transmembrane protein 2
51643	TMBIM4	Transmembrane BAX inhibitor motif containing 4
517	ATP5G2	ATP synthase, H^+ transporting, mitochondrial F0 complex, subunit C2 (subunit 9)
5265	SERPINA1	Serpin peptidase inhibitor, clade A (alpha-1 antiproteinase, antitrypsin), member 1
5355	PLP2	Proteolipid protein 2 (colonic epithelium-enriched)
5446	PON3	Paraoxonase 3
54657	UGT1A4	UDP glucuronosyltransferase 1 family, polypeptide A4
54658	UGT1A1	UDP glucuronosyltransferase 1 family, polypeptide A1
5479	PPIB	Peptidylprolyl isomerase B (cyclophilin B)
563	AZGP1	Alpha-2-glycoprotein 1, zinc-binding
56851	C15orf24	Chromosome 15 open reading frame 24
57817	HAMP	Hepcidin antimicrobial peptide
5950	RBP4	Retinol binding protein 4, plasma
6048	RNF5	Ring finger protein 5
6522	SLC4A2	Solute carrier family 4, anion exchanger, member 2 (erythrocyte membrane protein band 3-like 1)
7905	REEP5	Receptor accessory protein 5
84975	MFSD5	Major facilitator superfamily domain containing 5
9204	ZMYM6	Zinc finger, MYM-type 6
967	CD63	CD63 molecule

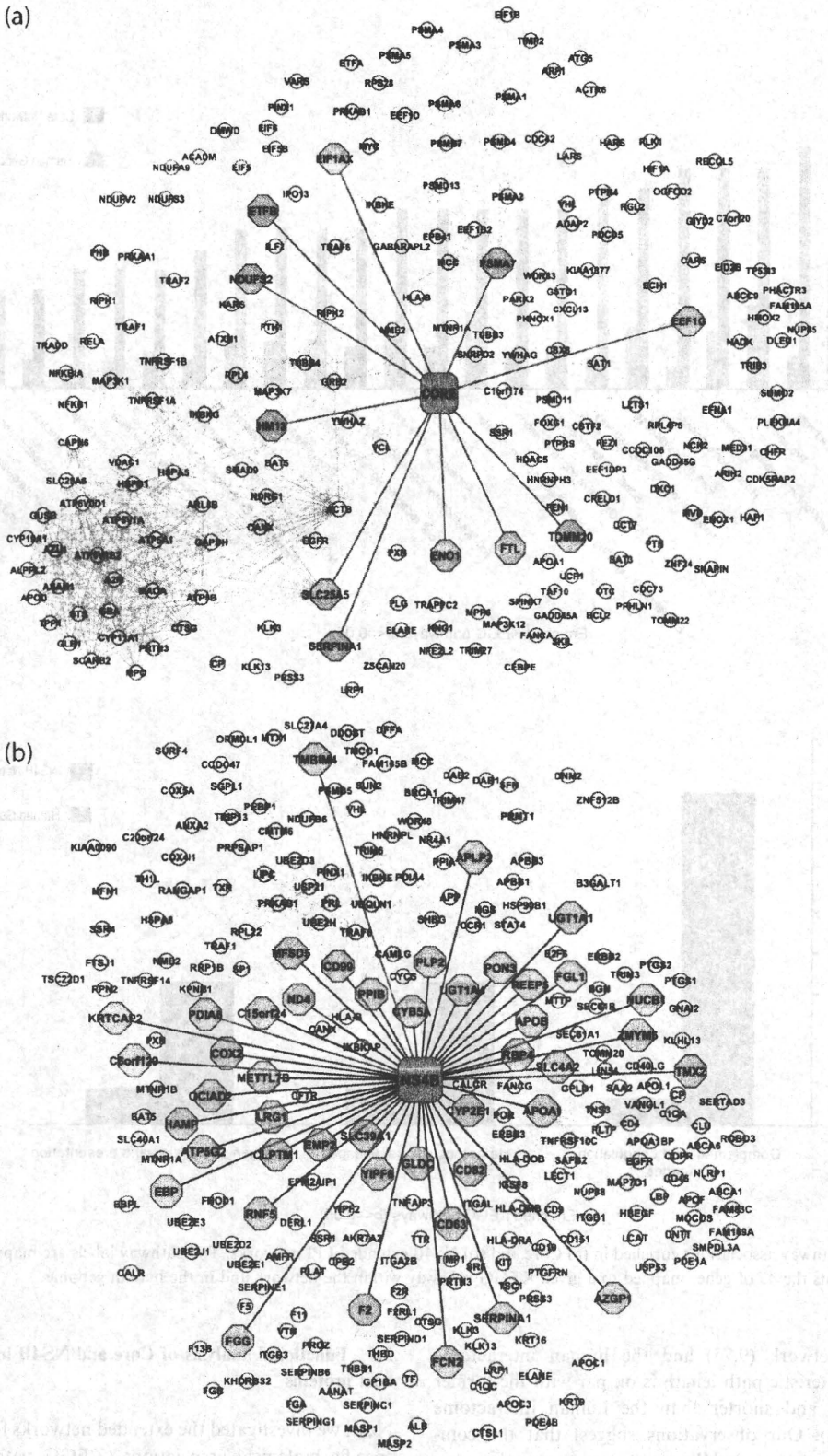

Fig. 1 Graphical representation of HCV (a) Core protein and (b) NS4B protein extended protein–protein interaction (PPI) networks. Red node: Core and NS4B protein; blue edge: Core and NS4B yeast two-hybrid (Y2H) interactions; green node: host proteins identified as interacting partners of Core and NS4B by Y2H membrane protein system; pink node: secondary interactors of the host proteins interacting with Core and NS4B; grey edge: interactions between human proteins. The node sizes differ for better clarity and do not reflect any topological attributes.

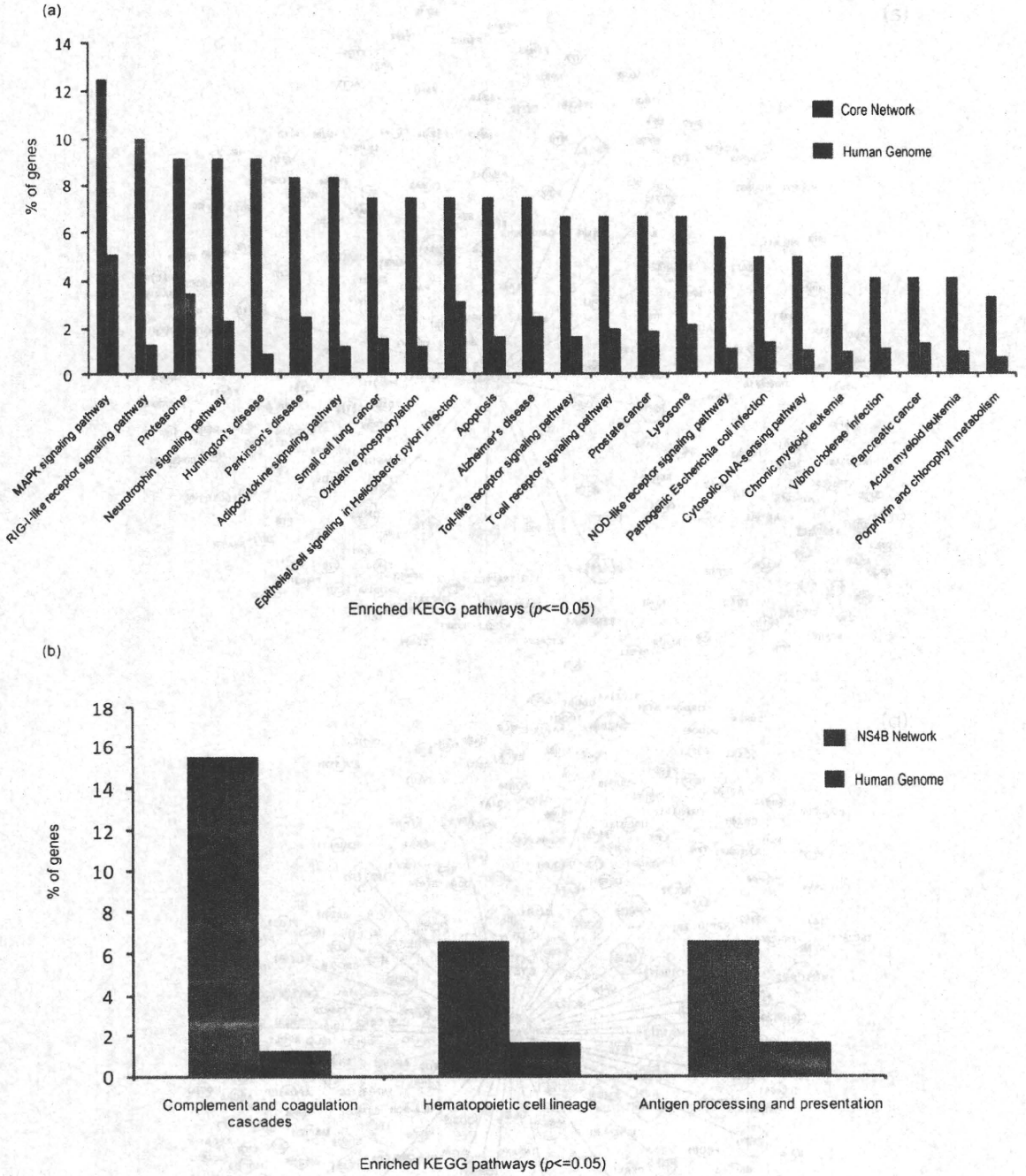

Fig. 2 KEGG pathway associations enriched in (a) Core and (b) NS4B extended PPI networks. The pathway labels are mapped to *x*-axis while the *y*-axis represents the % of genes mapped to a given KEGG pathway within the network and in the human genome.

Core MY2H network (9.75) and the human interactome (9.3), the characteristic path length is on par with the former (3.3 *versus* 2.9) and shorter than the human interactome (3.3 *versus* 4.04). Our observations suggest that the compactness of Core and NS4B interaction networks may facilitate rapid propagation of signaling information and allow the virus to respond rapidly to host mobilisation against HCV infection.

2.3 Functional analysis of Core and NS4B interactions with host proteins

Next, we investigated the extended networks for enrichment of specific biological associations (KEGG pathways,[24] OMIM phenotypes[25] and Gene Ontology [GO][26] terms). The analysis revealed that Core and NS4B protein networks were enriched in largely non-overlapping functional associations, indicating

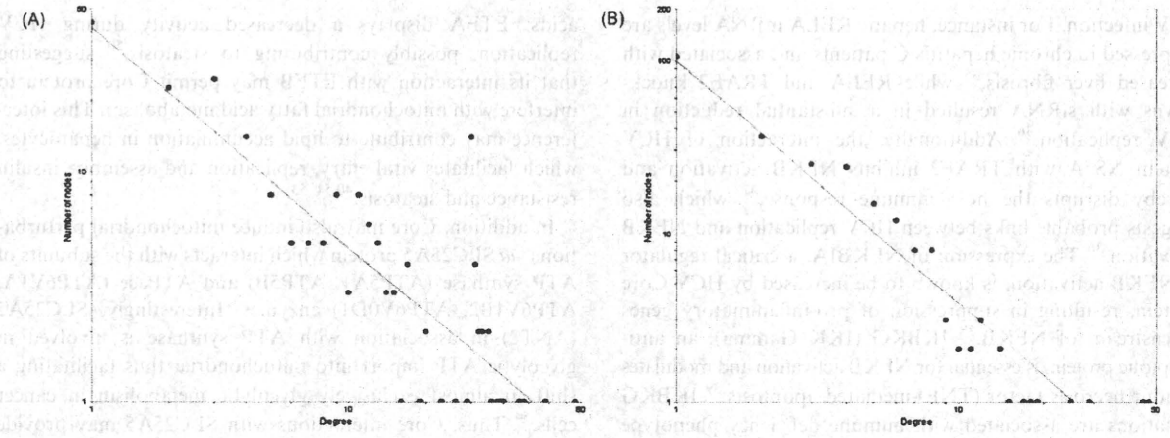

Fig. 3 Graphical representation of node degree distribution for Core and NS4B extended PPI networks. The node degree k is represented on the x-axis while the number of nodes mapped to a specific degree is represented on y-axis. The inverse trend between degree distribution and the number of proteins indicates a non-random network. The graphs correspond to (A) Core extended PPI network (R-squared value 0.727) and (B) NS4B extended network (R-squared value 0.895).

that they occupy different niches in HCV infection (Table 2; Fig. 2). Below, we first describe our observations on the Core network followed by the NS4B network.

2.3.1 Functional analysis of Core interaction network. The analysis of the extended Core interaction network revealed an enrichment of 24 KEGG pathways ($p \leq 0.05$) (Table 2), encompassing host immune response and oxidative and non-oxidative metabolism, which are likely to be significantly affected by HCV infection. Seventeen of the 24 enriched

Table 2 The number of proteins mapped to KEGG pathways significantly enriched ($p \leq 0.05$) in Core and NS4B extended PPI networks

KEGG pathway	Core network	NS4B network
Complement and coagulation cascades	—	21
MAPK signaling pathway	15	—
RIG-I-like receptor signaling pathway	12	—
Huntington's disease	11	—
Neurotrophin signaling pathway	11	—
Proteasome	10	—
Adipocytokine signaling pathway	10	—
Parkinson's disease	9	—
Alzheimer's disease	9	—
Antigen processing and presentation	—	9
Apoptosis	9	—
Epithelial cell signaling in *Helicobacter pylori* infection	9	—
Hematopoietic cell lineage	—	9
Oxidative phosphorylation	9	—
Small cell lung cancer	9	—
Lysosome	8	—
Prostate cancer	8	—
T cell receptor signaling pathway	8	—
Toll-like receptor signaling pathway	8	—
NOD-like receptor signaling pathway	7	—
Chronic myeloid leukemia	6	—
Cytosolic DNA-sensing pathway	6	—
Pathogenic *Escherichia coli* infection	6	—
Acute myeloid leukemia	5	—
Pancreatic cancer	5	—
Vibrio cholerae infection	5	—
Porphyrin and chlorophyll metabolism	4	—

associations overlapped with the enriched KEGG pathway associations inferred for the Core de Chassey network (Table S4, ESI†). Furthermore, to assess the robustness of enriched KEGG pathway associations, we explored the overlap of PPIs in the Core network with those documented in the I2D database.[27] We observed that 559 of the 1052 secondary interactions (see Material and Methods) in the Core interaction network were represented in I2D; the genes associated with these interactions were mapped to 22 enriched KEGG pathways, of which 20 were shared with the enriched KEGG pathway associations for the Core interaction network (data not shown).

2.3.1.1 Immune response. Immune response to HCV infection includes the recognition of the HCV RNA and proteins as pathogen associated molecular patterns (PAMPs) by macrophages and dendritic cells expressing germline-encoded pattern-recognition receptors (PRRs) such as Toll-like receptors (TLRs) and RIG-I-like receptors (RLRs), a family of RNA helicases. These events induce the production of Type I interferons (IFN-α/β) and inflammatory cytokines in the infected hepatocytes, which then activate downstream processes such as T-cell signalling for viral clearance.[28–32] The persistence of HCV in the host is attributed to its ability to hinder and evade the host immune response, which is regulated by the interplay between the HCV proteins and the components of the host immune system.[31,33,34]

Analysis of the Core interaction network revealed that six of the 11 Core interacting proteins interact with proteins mapped to one or more of the following KEGG pathways: "RIG-I-like receptor signaling" (12 of 208, $p = 4.0117 \times 10^{-7}$), "T cell receptor signaling" (8 of 208, $p = 0.0072$), "NOD-like receptor signaling" (7 of 208, $p = 0.00267$), "Toll-like receptor signaling" (8 of 208, $p = 0.0054$) and "Adipocytokine signaling" (10 of 208, $p = 1.637 \times 10^{-5}$). All of these pathways are related to innate and adaptive immunity (Fig. 1a and 4a, Table 2, Table S3, ESI†). Thus, Core protein may partly cause perturbations in the host immune response by virtue of these interactions. Several genes involved in these processes are implicated in

HCV infection. For instance, hepatic RELA mRNA levels are suppressed in chronic hepatitis C patients and associated with increased liver fibrosis,[35] while RELA and TRAF2 knockdowns with siRNA resulted in a substantial reduction in HCV replication.[36] Additionally, the interaction of HCV protein NS5A with TRAF2 inhibits NFKB activation and thereby disrupts the host immune response,[37] which also suggests probable links between HCV replication and NFKB activation.[36] The expression of NFKBIA, a critical regulator of NFKB activation, is known to be increased by HCV Core protein, resulting in suppression of pro-inflammatory genes downstream of NFKB.[38] IKBKG (IKK Gamma), an anti-apoptotic protein, is essential for NFKB activation and modulates tumour necrosis factor (TNF)-mediated apoptosis.[39] IKBKG mutations are associated with immune deficiency phenotype (Table S5, ESI†) and disruption of IKBKG activity may contribute to impaired immune response in HCV infection.

Some genes (PRKAA1 and PRKAB1) associated with the pro-inflammatory "Adipocytokine signaling pathway" also function in "Insulin signaling pathway", the disruption of which may contribute to insulin resistance (IR). IR is commonly observed in HCV infection and is associated with steatosis and fibrosis progression and impaired response to interferon-α anti-HCV therapy[40,41] and overexpression of HCV Core protein can induce IR in transgenic mice.[42] PRKAA1 expression is implicated in HCV infection,[43] suggesting that it may function in Core-induced IR.

The bulk of these genes (RELA, NFKB1, IKBKG, NFKBIA, TRAF2, PRKAA1) interact with SLC25A5 (Fig. 4a), suggesting that SLC25A5 may play an important role in Core perturbation of host innate immune response and liver fibrosis and possibly HCV replication.

2.3.1.2 Oxidative stress. HCV and other pathogens have evolved mechanisms to modulate host metabolism to facilitate their survival and propagation. ER stress, oxidative stress and mitochondrial dysfunction are some characteristic features associated with chronic hepatitis C infection.[44–46] Overexpression of HCV Core, NS3 and NS5A proteins is associated with increased production of reactive oxygen species (ROS), disrupted mitochondrial electron transport and altered Ca^{2+} homeostasis leading to perturbed Cytochrome c release from the mitochondria. This reaction together with induced insulin resistance eventually leads to accelerated fibrosis, HCC and DNA damage, while ensuring cell survival.[1,46–48]

Our Y2H screening identified NDUFS2, a mitochondrial protein essential for NADH to ubiquinone electron transfer, and ETFB, a mitochondrial electron-transfer flavoprotein as interacting partners of Core protein (Table 1). These interactions may permit Core protein to perturb oxidative electron transfer and consequently induce mitochondrial aberrations, which would be consistent with oxidative modification of mitochondrial respiratory complexes in pathogen infection.[49] Mutations in NDUFS2 (KEGG pathway "Oxidative phosphorylation" (10 of 208, $p = 0.0072$)) are associated with the OMIM phenotype "Mitochondrial complex I deficiency" (Table S5, ESI†), which causes several clinical disorders including liver disease. ETFB and its interacting partner ETFA are involved in beta-oxidation of fatty acids; ETFA displays a decreased activity during HCV replication, possibly contributing to steatosis,[50] suggesting that its interaction with ETFB may permit Core protein to interfere with mitochondrial fatty acid metabolism. This interference may contribute to lipid accumulation in hepatocytes, which facilitates viral entry, replication and assembly, insulin resistance and steatosis.[40,51–53]

In addition, Core may also induce mitochondrial perturbations *via* SLC25A5 protein which interacts with the subunits of ATP synthase (ATP5A1, ATP5B) and ATPase (ATP6V1A, ATP6V1B2, ATP6V0D1) enzymes. Interestingly, SLC25A5 (ANT2) in association with ATP synthase is involved in glycolytic ATP import into mitochondria, thus facilitating a shift to almost exclusively glycolytic metabolism in cancer cells.[54] Thus, Core interactions with SLC25A5 may provide an important link between oxidative stress and a shift in energy metabolism in HCV infection (see below).

2.3.1.3 Host energy metabolism and cell adhesion. HCV induction of oxidative stress is accompanied by a shift towards non-oxidative glucose metabolism to facilitate viral growth and is often characterised by elevated levels of glycolytic enzymes in the infected cells.[22,55] Our Y2H screening identified a novel interaction between Core protein and Alpha Enolase (ENO1), a key enzyme in the glycolytic pathway implicated in several disorders including metastatic cancer.[56] ENO1 was upregulated in response to HCV infection[22] and may be a key regulator in the shift towards glycolytic metabolism and viral replication. However, there is little understanding of the role of ENO1 in HCV infection and to the best of our knowledge no physical interaction between HCV proteins and ENO1 had been reported earlier.

Our network analysis revealed that some proteins interacting with ENO1 (ACTB, PXN) mapped to KEGG "Focal adhesion" pathway (Fig. 4b; Table 1, Table S3, ESI†). Focal adhesion regulates cell migration and its deregulation is linked to tumour progression and probably HCV propagation in the host.[7] Paxillin (PXN) is involved in cytoskeleton remodelling and a disruption in its activity by human papilloma virus (HPV) E6 protein is an important aspect of HPV pathogenesis.[57] Thus, the Core interaction with ENO1 may be important in HCV mediated cytoskeleton remodelling to facilitate viral propagation. SLC25A5 (ANT2), also implicated in cancer cell glycolysis,[54] interacts with proteins (ACTB, EGFR, PXN, VCL) involved in "Focal adhesion" (Fig. 4b; Table 1, Table S3, ESI†). Most of these interactions are associated with reasonable confidence levels.[58,59] Enhancement of EGFR signalling by HCV NS3/4A and NS5A proteins is important for viral replication and persistence.[60,61] Interestingly, EGFR is upregulated in lymph node metastasis in HCC, while SLC25A5 levels are downregulated,[20] suggesting that the Core interaction with SLC25A5 may be involved in regulating EGFR activity and host energy metabolism and consequently HCV replication and propagation.

HCV infection is also characterised by elevated hepatic iron levels (induced by ROC), which contributes to abnormalities in glucose metabolism and induction of insulin resistance, eventually leading to fibrosis.[62,63] Our Y2H screening identified interaction between Core and FTL, a subunit of the

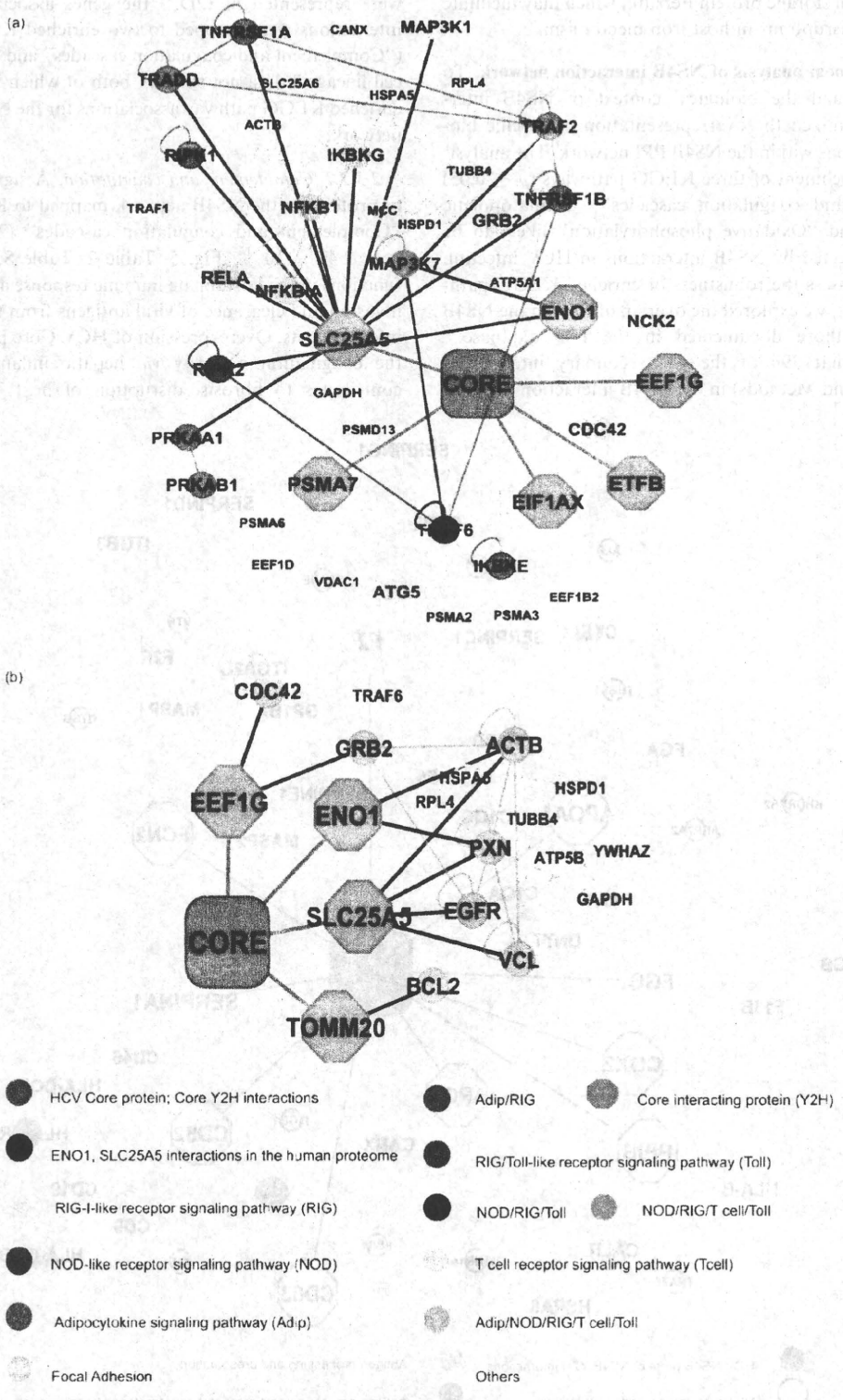

Fig. 4 Functional associations of the Core network. (a) Network illustration of interactions between HCV Core interacting proteins and host proteins mapped to five KEGG pathways— "RIG-I-like receptor signaling", "T cell receptor signaling", "NOD-like receptor signaling", "Toll-like receptor signaling" and "Adipocytokine signaling". SLC25A5 and ENO1 interactions are highlighted in black. (b) Network illustration of interactions between HCV Core interacting proteins and host proteins mapped to KEGG "Focal adhesion" pathway. The node sizes differ for better clarity and do not reflect any topological attributes.

intracellular iron storage protein Ferritin, which may facilitate Core induced disruptions in host iron metabolism.

2.3.2 Functional analysis of NS4B interaction network. To further understand the biological context of NS4B interactions, we examined the overrepresentation of specific biological associations within the NS4B PPI network. The analysis revealed an enrichment of three KEGG pathways ($p \leq 0.05$) "Complement and coagulation cascades", "Hematopoietic cell lineage" and "Oxidative phosphorylation" likely to be significantly affected by NS4B interactions in HCV infection (Table 2). To assess the robustness of enriched KEGG pathway associations, we explored the overlap of PPIs in the NS4B network with those documented in the I2D database.[27] We observed that 396 of the 436 secondary interactions (see Materials and Methods) in the NS4B interaction network were represented in I2D;[27] the genes associated with these interactions were mapped to two enriched KEGG pathways ("Complement and coagulation cascades" and "Hematopoietic cell lineage"; data not shown), both of which were among the enriched KEGG pathway associations for the NS4B interaction network.

2.3.2.1 Complement and coagulation. A significant number of proteins in the NS4B network mapped to KEGG pathway "Complement and coagulation cascades" (21 of 254, 5%; $p = 2.49 \times 10^{-14}$; Fig. 5, Table 2, Table S3, ESI†), which functions in the host innate immune response against pathogen invasion and clearance of viral antigens from the blood of the infected hosts. Overexpression of HCV Core protein activates the coagulation pathway *via* hepatic inflammation, which contributes to fibrosis, disruption of host T-cell mediated

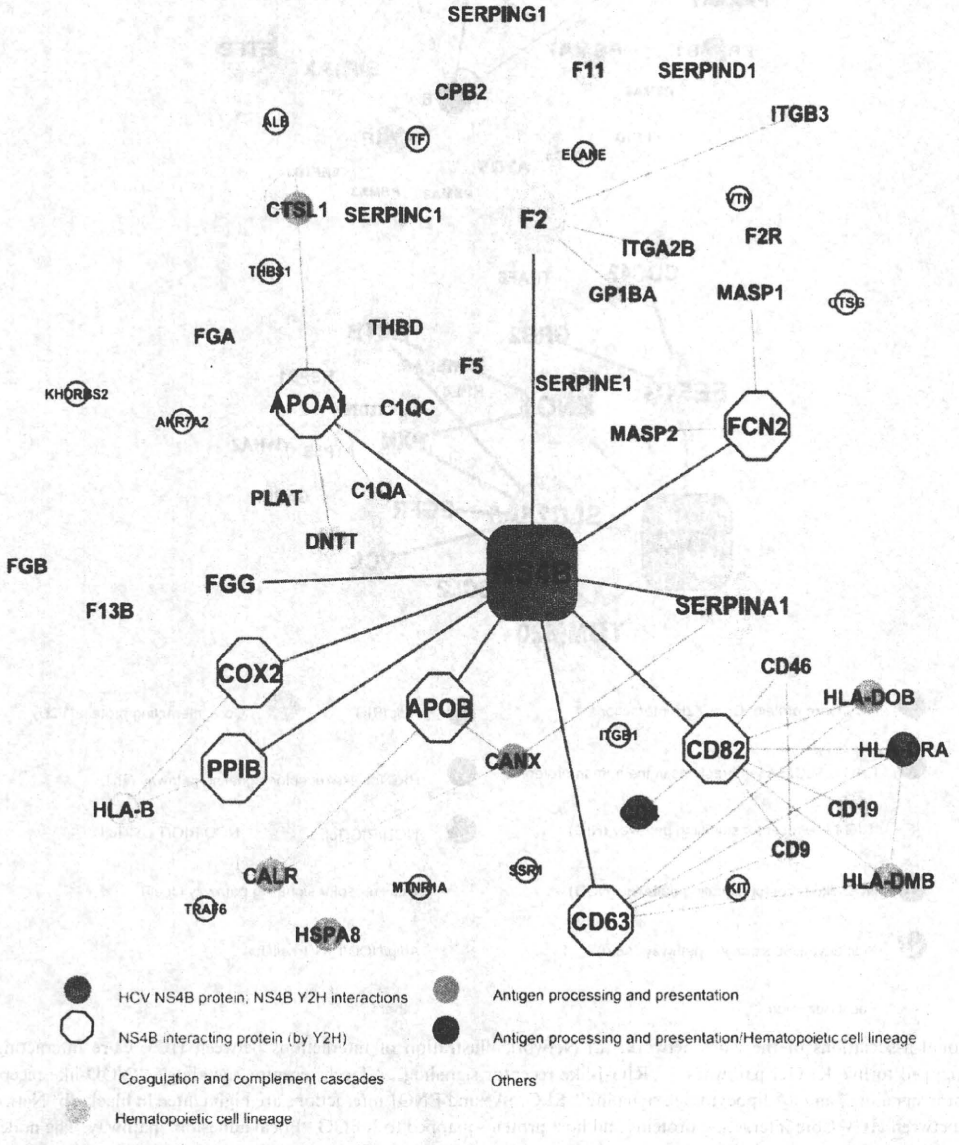

Fig. 5 Network illustration of HCV NS4B interactions associated with KEGG pathways Complement and coagulation cascades, Hematopoietic cell lineage and Antigen processing and presentation. The node sizes differ for better clarity and do not reflect any topological attributes.

immune response and viral persistence. Blocking complement activation can ameliorate the effects of HCV induced hepatic inflammation, suggesting the complement pathway as an attractive target for anti-HCV therapy.[64 67]

Our Y2H screening identified thrombin (F2), serine protease inhibitor SERPINA1 and fibrinogen gamma chain (FGG) as primary interacting partners of NS4B (Table 1, Fig. 2 and 5). Thrombin is implicated in liver cell fibrosis by inducing hepatic stellate cell proliferation,[68] while SERPINA1 defects are implicated in chronic liver disease, hepatitis C and HCC[69 71] and elevated FGG expression and plasma fibrinogen levels are associated with HCC progression.[72] To the best of our knowledge, however, no interactions between these proteins and NS4B had been reported earlier. Interactions with thrombin and SERPINA1 may allow NS4B to directly perturb the host immune response *via* complement activation and thus contribute to HCV pathogenesis and HCC.

2.3.2.2 Hematopoietic development and antigen presentation. Chronic HCV infection induces a reduced natural killer (NK) cell frequency and activity, resulting in impaired cytokine secretion, a stunted immune response and viral persistence.[73] Analysis of the NS4B network revealed an enrichment of proteins (9 of 254, 4%; $p = 0.0213$) mapped to KEGG pathway "Hematopoietic cell lineage", which functions in the generation of NK cells and T and B lymphocytes. The T and B lymphocytes play an important role in innate and adaptive immune response.[74] Our analysis suggested that interactions with host proteins CD63, CD82 and APOA1 (Apolipoprotein A-I) that physically interact with the components of "Hematopoietic cell lineage" may permit NS4B to influence and possibly impair NK cell development and host immune response (Fig. 5).

We also observed an enrichment of proteins (9 of 254, 4%; $p = 0.0155$) mapped to the KEGG pathway "Antigen processing and presentation". Our network analysis showed that these proteins interact with four NS4B interacting proteins: CD63 and CD82 (interacting with HLA-DMB; HLA-DOB and HLA-DRB); APOB (Apolipoprotein B; interacting with CALR, CANX and HSPA8) and APOA1 (interacting with CTSL1 and DNTT) (Fig. 5). The dysfunction of CD63 and CD82 is implicated in cell-to-cell transmission of HIV-1,[75] suggesting that their interaction with NS4B may be crucial to the spread of HCV in the host. APOB associated cholesterol is positively associated with HCV assembly and entry[76,77] thus, NS4B interactions with APOB (and possibly APOA1) may modulate host lipid metabolism and immune response to facilitate HCV pathogenesis and steatosis.[16]

2.3.2.3 Oxidative stress. NS4B overexpression induces ER stress, unfolded protein response (UPR) and production of ROS, which eventually triggers oxidative stress.[78] However, whether NS4B may induce mitochondrial dysfunction by direct associations remains unclear.

Our Y2H screening identified three mitochondrial proteins COX2 (MT-CO2; Cytochrome c oxidase II), ND4 (mitochondrially encoded NADH dehydrogenase 4) and ATP5G2 (ATP synthase subunit C2) to interact with NS4B (Table 1). These proteins map to the KEGG pathway "Oxidative phosphorylation" and are components of the mitochondrial oxidative machinery. Disruptions in ND4 activity[79] and Cytochrome c oxidase deficiency[80] are associated with oxidative stress. Thus, NS4B interactions with the mitochondrial oxidative machinery may allow the virus to influence host oxidative metabolism and potentially induce insulin resistance, steatosis and fibrosis.

The analysis of NS4B interactions may help unravel further associations in HCV infection. Our Y2H screening identified RBP4 (retinol binding protein 4; Table 1) to interact with NS4B, which is suggested to be inversely correlated with chronic HCV infection.[81] However, a precise understanding of the significance of the interactions identified here would be apparent only with further experimental investigations.

2.4 Validation of novel interactions for their role in HCV replication and release

Traditionally, viral and host proteins associated with various steps in HCV lifecycle (internalisation, replication, assembly and release) have been the primary targets in studies focused on anti-HCV strategies. Due to the lack of a suitable model system for HCV infection, cell culture-based systems for HCV RNA replication and infectious viral particle production have been extensively exploited to understand HCV–host interactions and identify potential anti-HCV drug targets.[4,82 84] Our observations by virtue of extended PPI networks suggested novel and potentially crucial roles of host proteins ENO1, PXN, SLC25A5 and VCL (vinculin), an important component of cell–cell junctions,[85] in HCV replication and persistence in the host.

To further explore the roles of these proteins in HCV life cycle, we performed cellular assays to assess the impact of ENO1, PXN, SLC25A5 and VCL siRNA knockdowns on HCV replication and release. Since HCV-production systems established with HCV JFH1 infectious strain (genotype 2a) isolates alone are capable of both efficient replication and production of infectious viral particles,[86,87] JFH1 was used to infect the Huh7OK1 cell line 24 h after transfection with each siRNA (see Materials and Methods). The infected cells were harvested after 72 h post-infection and the expression of each host protein was assessed by qRT-PCR (Fig. 6A). Supernatant viral RNA was significantly decreased by the knockdown of ENO1, but was not affected by the knockdown of PXN in the infected cells, while SLC25A5 knockdown resulted in a slight but statistically significant increase in the amount of the supernatant viral RNA (Fig. 6B). Intracellular viral RNA was significantly reduced by the knockdown of ENO1, but was unaffected by the knockdown of PXN and SLC25A5 (Fig. 6C), suggesting that ENO1 and SLC25A5 regulate HCV replication and assembly/secretion, respectively. VCL knockdown had no significant effect on the intracellular and supernatant virus RNA in the infected cells (data not shown).

To assess the impact of the knockdown of these genes on other HCV genotypes, we repeated the HCV replication assays using Huh-7 cells including HCV replicons derived from JFH1 and Con1 (genotype 1b) infectious strains. Unlike Huh7OK1 cells infected with JFH1, these replicon systems facilitate studies on HCV replication but not infectious virus

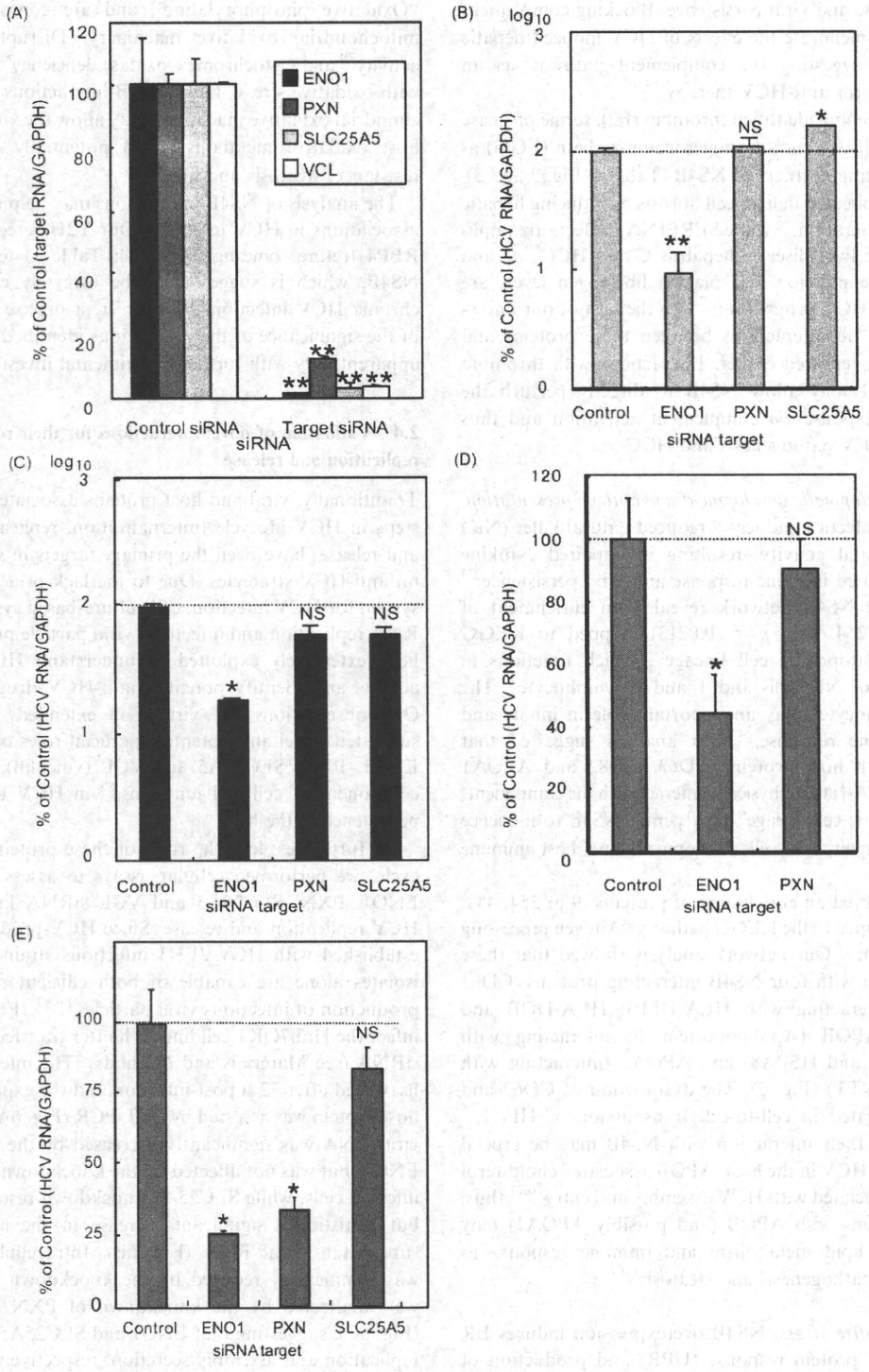

Fig. 6 Effects of knockdown of host protein candidates on HCV propagation and replication. Host proteins ENO1, PXN, SLC25A5 and VCL were suppressed by RNAi in Huh7OK1 cells infected with HCV JFH1 strain (genotype 2a; A, B and C) and in Huh-7 cells including JFH1 replicon RNA (D) or Con1 replicon (genotype 1b; E). Amounts of mRNA of the intracellular host proteins (A), the supernatant viral RNA (B) and the intracellular viral RNA (C, D and E) were estimated. Each value was represented as the percentage of the corresponding quantity measured for the cells transfected with the control siRNA. $*P < 0.05$; $**P < 0.01$; NS: not statistically significant.

secretion.[88] ENO1 knockdown suppressed HCV replication in Huh-7 cells, including either subgenomic replicon RNA of JFH1, which does not encode structural proteins (Fig. 6D), or of Con1, which encodes all viral proteins (Fig. 6E). On the other hand, PXN knockdown in Huh-7 cells including Con1 impaired HCV replication significantly (Fig. 6E), in contrast

to no effect in HuhOK1 cells including JFH1, as described above. This result was not due to the differences in cell lines and the expression of Core protein, because PXN knockdown in Huh-7 cells including JFH1 had no significant effect on intracellular HCV RNA production (Fig. 6D). This observation suggests that PXN possibly regulates the replication of HCV genotype 1b but not of genotype 2a. The standard therapy of pegylated interferon-α plus rebavirin treatment typically achieves less than 50% sustained virological response in HCV genotype 1b infected patients compared to 80% in genotype 2 and 3 infected patients.[89] Therefore, the identification of novel specific (PXN) and non-specific (ENO1) regulators of replication in different HCV genotypes provides potentially attractive targets for developing more effective combinatorial therapies with interferon/RBV treatment.

3. Conclusions

We describe here our observations of PPIs between HCV encoded and host proteins. We first derived a set of experimentally determined interactions between HCV proteins Core and NS4B and host proteins *via* Y2H screens customised for detecting membrane protein interactions. We proceeded to map these interactions onto an overall interaction network that comprised a repertoire of connections potentially required for the two viral proteins to link up with and modulate the components of the host cellular networks. We then employed a network-based approach to further understanding the biological context of these connections in HCV pathogenesis. Core interacting protein SLC25A5 manifested as a potentially important link between the Core protein and the host immune machinery. ENO1, by virtue of gathered interactions, may also function in regulating HCV replication and propagation. We identified 45 previously uncharacterised interactions for NS4B protein that may be crucial for NS4B to function as an important hub in HCV–host interactions. Further investigation of these interactions may help expand substantially our understanding of NS4B function in viral pathogenesis and its potential as an anti-HCV target.

Our observations were then used to prioritise four of the 459 potential candidates in the two extended PPI networks for follow-up experimental investigations through cellular assays based on siRNA knockdowns for HCV genotypes 1b and 2a. These assays validated Core interacting protein ENO1 as a novel regulator of HCV replication and a potentially minor role of SLC25A5 in HCV secretion. In addition, our assays also suggested a genotype 1b specific role of the host protein PXN (which interacts with ENO1 and SLC25A5) in HCV replication. These observations highlighted the attractiveness of the selected host proteins as suitable targets in potentially more effective targeted anti-HCV strategies. The genetic variability of HCV has facilitated the emergence of drug resistance against antiviral drugs that target HCV components. Therefore, antivirals that target less mutable host proteins critical to viral pathogenesis, preferably with minimal adverse side effects, may provide attractive alternatives to existing therapies. That we were able to experimentally validate three of the four genes selected for experimental characterisation reinforces the strengths of elaborate network-based approaches employing diverse functional associations and knowledge-based inputs for identification and prioritisation of suitable targets for experimental and therapeutic investigation. Our study also provides a generic framework for investigating host–pathogen interactions. Such investigation may help identify common themes associated with pathogen (especially viral) infection and help develop effective broad spectrum strategies aimed at ameliorating pathogen (viral) infections.

4. Materials and methods

4.1 Y2H membrane protein assay

Screening for the genes encoding the host proteins that interact with HCV Core and NS4B proteins derived from genotype 1b Con1 strain was performed with a Y2H membrane protein kit system (MoBiTec, Göttingen, Germany) as per the manufacturers specifications. Human adult liver libraries that were constructed based on pPR3 were purchased from MoBiTec and expressed as a fusion protein fused to the N-terminal or the C-terminal end of Nub-G. The cDNA of the Core (or NS4B) encoding region of the HCV polyprotein from the Con1 strain (genotype 1b) was amplified by polymerase chain reaction (PCR) and cloned into the pBT3-N vector (MoBiTec). The screening process was repeated three times to maximise the confidence in the interactions. The total number of screened transformants was 4×10^6, which is about twice the amount of independent clones in the libraries employed for the screening. The clones including genes encoding the Core (or NS4B) interacting proteins were grown on the histidine- and adenosine-deficient culture plate containing a high concentration (10 mM) of 3-amino-1,2,4-triazole (3AT), to remove weak interactions and minimise false positive data. The positive colonies were identified from the blue colour by beta-galactosidase assay (data not shown).

4.2 PPI resources

Secondary interactors of the Core and NS4B interacting proteins were retrieved from BioGRID[90] (version 2.0.63) and PPIView[91] databases. These secondary interactions were merged, filtered for redundancy and appended to the Y2H interactions to infer an extended PPI network. To estimate the robustness of the interactions employed to construct extended PPI networks and infer enriched functional associations (see below), we examined the Human PPI dataset from the I2D database[27] for its overlap with the BioGRID[90]- and PPIView[91]-derived secondary interactions.

4.3 Network topology analysis

Network components were visualised using Cytoscape 2.6,[92] while the network properties such as *node degree distribution* and *average shortest path* measures were computed using Cytoscape NetworkAnalyzer plugin.[93] The degree of node v is defined as the number of nodes directly connected to it, *i.e.*, its first neighbours. Node degree distribution $P(k)$ is the number of nodes with a degree k for $k = 0,1,2\ldots$. By fitting a line on datasets, such as node degree distribution data, the

pattern of their dependencies can be visualised. NetworkAnalyzer considers only data points with positive coordinate values for fitting the line where the power law curve of the form $y = \beta x^{a}$ is transformed into a linear model $\ln y = \ln \beta + a \ln x$ and the *R*-squared value (coefficient of determination) is computed on logarithmised data, which provides a measure of how well the data points fit to the curve. The *average shortest path length*, also known as the *characteristic path length*, gives the expected distance between two connected nodes.

4.4 Functional analysis by characterisation of enriched biological associations

GO associations retrieved from the GO consortium,[26] biological pathway data from KEGG[24] and disease phenotype associations from OMIM[25] were used to assign functional annotations to the genes in the extended networks. The enrichment of specific biological associations within each network was estimated by Fisher's exact test ($p \leq 0.05$) using the module fisher.test from the R statistical package (http://www.R-project.org). The inferred *p*-values were further adjusted for multiple test correction to control the false discovery rate using the Benjamini and Hochberg procedure.[94,95]

4.5 RNAi and transfection

The siRNA pair targets to ENO1, PXN and SLC25A5 and VCL were purchased from Ambion (Ambion, Austin, TX). Stealth™ RNAi Negative Control Low GC Duplex (Invitrogen) was used as a control siRNA. Each siRNA duplex was introduced into the cell lines using lipofectamine RNAiMax (Invitrogen, Carlsbad, CA). Ambion ID numbers of siRNA duplex of ENO1, PXN, SLC25A5 and VCL were S4682, S44629, S1375 and S14764, respectively. The replicon cell line, described below, was transfected with each siRNA at a final concentration of 20 nM as per the manufacturer's protocol and then seeded at 2.5×10^4 cells per well of a 24-well plate. The transfected cells were harvested at 72 h posttransfection. The Huh7OK1 cell line, described below, was transfected with each siRNA at a final concentration of 20 nM as per the manufacturer's protocol and then seeded at 2.5×10^4 cells per well of a 24-well plate. The transfected cells were infected with HCV JFH1 infectious strain (genotype 2a) at a MOI of 0.05 at 24 h posttransfection. The resulting cells were harvested at the indicated times.

4.6 Quantitative reverse-transcription PCR (qRT-PCR)

Total RNA was prepared from cell and culture supernatant using the RNeasy mini kit (QIAGEN) and QIAamp Viral RNA Mini Kit (QIAGEN), respectively. First-strand cDNA was synthesised using High capacity cDNA reverse transcription kit (Applied Biosystems, Carlsbad, CA) with random primers. Each cDNA was estimated by Platinum SYBR Green qPCR Super Mix UDG (Invitrogen) as per the manufacturer's protocol. Fluorescent signals of SYBR Green were analysed with ABI PRISM 7000 (Applied Biosystems). The HCV internal ribosomal entry site (IRES) region and human glyceraldehyde-3-phosphate dehydrogenase (GAPDH) gene were amplified with the primer pairs 5′-GAGTGTCGTGCAGCCTCCA-3′ and 5′-CACTCGCAAGCACCCTATCA-3′, and 5′-GAAGGTCGGAGTCAACGGATT-3′ and 5′-TGATGACAAGCTTCCCGTTCTC-3′, respectively.[96] The quantities of the HCV genome and other host mRNAs were normalised with that of GAPDH mRNA. ENO1, PXN, and SLC25A5 genes were amplified using the primer pairs 5′-TGCCTCCTGCTCAAAGTCAACCAGA-3′ and 5′-GGTTTCTGAAGTTCCTGCCGGCAAA-3′; 5′-TACTGTCGCAAGGACTACTTCGAC-3′ and 5′-AAGAAGCTGCCGTTCACGAATG-3′; 5′-AGTCTGCCTCCTCTTTCAACATGAC-3′ and 5′-GGACCACGCAGTCTATAATGCCTTT-3′, respectively. VCL gene was amplified using the primer pair 5′-GGTATTTGATGAGAGGGCAGCTAAC-3′ and 5′-GGCTGAATGTTGGCCATAGCTAC-3′.

4.7 Cell lines and virus infection

Cells from the Huh7OK1 cell line are highly permissive to HCV JFH1 strain (genotype 2a) infection compared to Huh 7.5.1 and exhibit highest propagation efficiency for JFH1.[96] These cells were maintained at 37 °C in humidified atmosphere and 5% CO_2, in Dulbecco's modified Eagle's medium (DMEM) (Sigma, St. Louis, MO) supplemented with nonessential amino acids (NEAA), sodium pyruvate, and 10% fetal calf serum (FCS). The human hepatoma cell line Huh-7, harbouring the full genome of HCV Con1 strain (genotype 1b), was prepared as described by Pietschmann *et al.*[88] We also established Huh-7 cell line harbouring the subgenome of the JFH1 strain by the transfection of the plasmid pSGR-JFH1.[97] The Huh7-derived cell lines harbouring a full length HCV replicon were maintained in DMEM containing 10% FCS, nonessential amino acids, sodium pyruvate and 1 mg ml^{-1} G418 (Nakarai Tesque, Tokyo, Japan). The viral RNA of JFH1 was introduced into Huh7OK1 as described by Wakita *et al.*[86] The viral RNA of JFH1 derived from the plasmid pJFH1 was prepared as described by Wakita *et al.*[86]

Acknowledgements

This study was supported by the Industrial Technology Research Grant Program in 2007 from New Energy and Industrial Technology Development Organization (NEDO) of Japan and also by grants-in-aid from the Ministry of Health, Labor, and Welfare; the Ministry of Education, Culture, Sports, Science, and Technology; the Osaka University Global Center of Excellence Program; and the Foundation for Biomedical Research and Innovation. We gratefully acknowledge Dr Tadashi Imanishi of Biomedicinal Information Research Centre (AIST) for providing us with the PPIview interactions and permission for publishing the data and Dr T. Wakita for providing us with cell lines and plasmids. We also thank Yi-An Chen for technical assistance.

References

1 H. Tang and H. Grise, *Clin. Sci.*, 2009, **117**, 49–65.
2 H. Myrmel, E. Ulvestad and B. Asjo, *APMIS*, 2009, **117**, 427–439.
3 K. Moriishi, R. Mochizuki, K. Moriya, H. Miyamoto, Y. Mori, T. Abe, S. Murata, K. Tanaka, T. Miyamura, T. Suzuki, K. Koike

and Y. Matsuura, *Proc. Natl. Acad. Sci. U. S. A.*, 2007, **104**, 1661–1666.
4 D. Moradpour, F. Penin and C. M. Rice, *Nat. Rev. Microbiol.*, 2007, **5**, 453–463.
5 M. D. Dyer, T. M. Murali and B. W. Sobral, *PLoS Pathog.*, 2008, **4**, e32.
6 T. Ideker and R. Sharan, *Genome Res.*, 2008, **18**, 644–652.
7 B. de Chassey, V. Navratil, L. Tafforeau, M. S. Hiet, A. Aublin-Gex, S. Agaugue, G. Meiffren, F. Pradezynski, B. F. Faria, T. Chantier, M. Le Breton, J. Pellet, N. Davoust, P. E. Mangeot, A. Chaboud, F. Penin, Y. Jacob, P. O. Vidalain, M. Vidal, P. Andre, C. Rabourdin-Combe and V. Lotteau, *Mol. Syst. Biol.*, 2008, **4**, 230.
8 S. L. Tan, G. Ganji, B. Paeper, S. Proll and M. G. Katze, *Nat. Biotechnol.*, 2007, **25**, 1383–1389.
9 P. Georgel, C. Schuster, M. B. Zeisel, F. Stoll-Keller, T. Berg, S. Bahram and T. F. Baumert, *Trends Mol. Med.*, 2010, **16**, 277–286.
10 M. A. Calderwood, K. Venkatesan, L. Xing, M. R. Chase, A. Vazquez, A. M. Holthaus, A. E. Ewence, N. Li, T. Hirozane-Kishikawa, D. E. Hill, M. Vidal, E. Kieff and E. Johannsen, *Proc. Natl. Acad. Sci. U. S. A.*, 2007, **104**, 7606–7611.
11 P. Uetz, Y. A. Dong, C. Zeretzke, C. Atzler, A. Baiker, B. Berger, S. V. Rajagopala, M. Roupelieva, D. Rose, E. Fossum and J. Haas, *Science*, 2006, **311**, 239–242.
12 K. Okamoto, Y. Mori, Y. Komoda, T. Okamoto, M. Okochi, M. Takeda, T. Suzuki, K. Moriishi and Y. Matsuura, *J. Virol.*, 2008, **82**, 8349–8361.
13 K. Moriishi, I. Shoji, Y. Mori, R. Suzuki, C. Kataoka and Y. Matsuura, *Hepatology*, 2010, **52**(2), 411–420.
14 J. Dubuisson, *World J. Gastroenterol.*, 2007, **13**, 2406–2415.
15 Y. Mori, K. Moriishi and Y. Matsuura, *Int. J. Biochem. Cell Biol.*, 2008, **40**, 1437–1442.
16 J. Gouttenoire, F. Penin and D. Moradpour, *Rev. Med. Virol.*, 2010, **20**(2), 117–129.
17 J. Snider, S. Kittanakom, D. Damjanovic, J. Curak, V. Wong and I. Stagljar, *Nat. Protoc.*, 2010, **5**, 1281–1293.
18 M. Kruger, C. Beger, P. J. Welch, J. R. Barber, M. P. Manns and F. Wong-Staal, *Mol. Cell. Biol.*, 2001, **21**, 8357–8364.
19 B. Schwer, S. Ren, T. Pietschmann, J. Kartenbeck, K. Kaehlcke, R. Bartenschlager, T. S. Yen and M. Ott, *J. Virol.*, 2004, **78**, 7958–7968.
20 C. F. Lee, Z. Q. Ling, T. Zhao, S. H. Fang, W. C. Chang, S. C. Lee and K. R. Lee, *World J. Gastroenterol.*, 2009, **15**, 356–365.
21 Y. Kuramitsu and K. Nakamura, *Expert Rev. Proteomics*, 2005, **2**, 589–601.
22 D. L. Diamond, A. J. Syder, J. M. Jacobs, C. M. Sorensen, K. A. Walters, S. C. Proll, J. E. McDermott, M. A. Gritsenko, Q. Zhang, R. Zhao, T. O. Metz, D. G. Camp, 2nd, K. M. Waters, R. D. Smith, C. M. Rice and M. G. Katze, *PLoS Pathog.*, 2010, **6**, e1000719.
23 C. Welsch, M. Albrecht, J. Maydt, E. Herrmann, M. W. Welker, C. Sarrazin, A. Scheidig, T. Lengauer and S. Zeuzem, *J. Mol. Graphics Modell.*, 2007, **26**, 546–557.
24 K. F. Aoki-Kinoshita and M. Kanehisa, *Methods Mol. Biol.*, 2007, **396**, 71–91.
25 J. H. U. B. McKusick-Nathans Institute of Genetic Medicine, MD and National Center for Biotechnology Information, National Library of Medicine (Bethesda, MD), 2010.
26 M. Ashburner, C. A. Ball, J. A. Blake, D. Botstein, H. Butler, J. M. Cherry, A. P. Davis, K. Dolinski, S. S. Dwight, J. T. Eppig, M. A. Harris, D. P. Hill, L. Issel-Tarver, A. Kasarskis, S. Lewis, J. C. Matese, J. E. Richardson, M. Ringwald, G. M. Rubin and G. Sherlock, *Nat. Genet.*, 2000, **25**, 25–29.
27 K. R. Brown and I. Jurisica, *GenomeBiology*, 2007, **8**, R95.
28 K. Hiroishi, T. Ito and M. Imawari, *J. Gastroenterol. Hepatol.*, 2008, **23**, 1473–1482.
29 T. Kawai and S. Akira, *Ann. N. Y. Acad. Sci.*, 2008, **1143**, 1–20.
30 T. Saito and M. Gale, Jr., *Hepatol. Res.*, 2008, **38**, 115–122.
31 G. Szabo and A. Dolganiuc, *Clin. Liver Dis.*, 2008, **12**, 675–692.
32 X. Zhang, J. Dou and M. W. Germann, *Med. Res. Rev.*, 2009, **29**, 843–866.
33 E. H. Sklan, P. Charuworn, P. S. Pang and J. S. Glenn, *Nat. Rev. Gastroenterol. Hepatol.*, 2009, **6**, 217–227.
34 D. R. Taylor and E. Silberstein, *Front. Biosci.*, 2009, **14**, 4950–4961.
35 P. Boya, E. Larrea, I. Sola, P. L. Majano, C. Jimenez, M. P. Civeira and J. Prieto, *Hepatology*, 2001, **34**, 1041–1048.
36 T. I. Ng, H. Mo, T. Pilot-Matias, Y. He, G. Koev, P. Krishnan, R. Mondal, R. Pithawalla, W. He, T. Dekhtyar, J. Packer, M. Schurdak and A. Molla, *Hepatology*, 2007, **45**, 1413–1421.
37 K. J. Park, S. H. Choi, S. Y. Lee, S. B. Hwang and M. M. Lai, *J. Biol. Chem.*, 2002, **277**, 13122–13128.
38 H. Nguyen, S. Sankaran and S. Dandekar, *Virology*, 2006, **354**, 58–68.
39 D. Legarda-Addison, H. Hase, M. A. O'Donnell and A. T. Ting, *Cell Death Differ.*, 2009, **16**, 1279–1288.
40 J. A. Del Campo and M. Romero-Gomez, *World J. Gastroenterol.*, 2009, **15**, 5014–5019.
41 M. W. Douglas and J. George, *World J. Gastroenterol.*, 2009, **15**, 4356–4364.
42 H. Miyamoto, K. Moriishi, K. Moriya, S. Murata, K. Tanaka, T. Suzuki, T. Miyamura, K. Koike and Y. Matsuura, *J. Virol.*, 2007, **81**, 1727–1735.
43 M. C. Ryan, P. V. Desmond, J. L. Slavin and M. Congiu, *Journal of Viral Hepatitis*, 2010, DOI: 10.1111/j.1365-2893.2010.01283.x.
44 C. Fierbinteanu-Braticevici, M. Mohora, D. Cretoiu, S. Cretoiu, A. Petrisor, R. Usvat and D. A. Ion, *Rom. J. Morphol. Embryol.*, 2009, **50**, 407–412.
45 S. Pal, S. J. Polyak, N. Bano, W. C. Qiu, R. L. Carithers, M. Shuhart, D. R. Gretch and A. Das, *J. Gastroenterol. Hepatol.*, 2010, **25**(3), 627–634.
46 C. Piccoli, G. Quarato, M. Ripoli, A. D'Aprile, R. Scrima, O. Cela, D. Boffoli, D. Moradpour and N. Capitanio, *Biochim. Biophys. Acta, Bioenerg.*, 2009, **1787**, 539–546.
47 T. Wang, R. V. Campbell, M. K. Yi, S. M. Lemon and S. A. Weinman, *Journal of Viral Hepatitis*, 2009, DOI: 10.1111/j.1365-2893.2009.01238.x.
48 M. Korenaga, T. Wang, Y. Li, L. A. Showalter, T. Chan, J. Sun and S. A. Weinman, *J. Biol. Chem.*, 2005, **280**, 37481–37488.
49 J. J. Wen and N. Garg, *Free Radical Biol. Med.*, 2004, **37**, 2072–2081.
50 R. Singaravelu, D. R. Blais, C. S. McKay and J. P. Pezacki, *Proteome Sci.*, 2010, **8**, 5.
51 M. Alaei and F. Negro, *Diabetes Metab.*, 2008, **34**, 692–700.
52 B. Bartosch, *J. Hepatol.*, 2009, **50**, 845–847.
53 G. H. Syed, Y. Amako and A. Siddiqui, *Trends Endocrinol. Metab.*, 2010, **21**, 33–40.
54 A. Chevrollier, D. Loiseau, B. Chabi, G. Renier, O. Douay, Y. Malthiery and G. Stepien, *J. Bioenerg. Biomembr.*, 2005, **37**, 307–316.
55 M. Ripoli, A. D'Aprile, G. Quarato, M. Sarasin-Filipowicz, J. Gouttenoire, R. Scrima, O. Cela, D. Boffoli, M. H. Heim, D. Moradpour, N. Capitanio and C. Piccoli, *J. Virol.*, 2010, **84**, 647–660.
56 H. J. Kang, S. K. Jung, S. J. Kim and S. J. Chung, *Acta Crystallogr., Sect. D: Biol. Crystallogr.*, 2008, **64**, 651–657.
57 J. W. Fei and E. M. de Villiers, *Int. J. Cancer*, 2008, **123**, 108–116.
58 O. K. Bernhard, A. L. Cunningham and M. M. Sheil, *J. Am. Soc. Mass Spectrom.*, 2004, **15**, 558–567.
59 C. L. de Hoog, L. J. Foster and M. Mann, *Cell (Cambridge, Mass.)*, 2004, **117**, 649–662.
60 E. D. Brenndorfer, J. Karthe, L. Frelin, P. Cebula, A. Erhardt, J. Schulte am Esch, H. Hengel, R. Bartenschlager, M. Sallberg, D. Haussinger and J. G. Bode, *Hepatology*, 2009, **49**, 1810–1820.
61 J. Mankouri, S. Griffin and M. Harris, *Traffic*, 2008, **9**, 1497–1509.
62 H. C. Isom, E. I. McDevitt and M. S. Moon, *Biochim. Biophys. Acta, Gen. Subj.*, 2009, **1790**, 650–662.
63 A. Lecube, C. Hernandez and R. Simo, *Diabetes/Metab. Res. Rev.*, 2009, **25**, 403–410.
64 C. L. Basiglio, S. M. Arriaga, F. Pelusa, A. M. Almara, J. Kapitulnik and A. D. Mottino, *Clin. Sci.*, 2009, **118**, 99–113.
65 V. Calvaruso, S. Maimone, A. Gatt, E. Tuddenham, M. Thursz, M. Pinzani and A. K. Burroughs, *Gut*, 2008, **57**, 1722–1727.
66 M. L. Chang, C. T. Yeh, D. Y. Lin, Y. P. Ho, C. M. Hsu and D. M. Bissell, *BMC Med. Genomics*, 2009, **2**, 51.
67 Z. Q. Yao, D. T. Nguyen, A. I. Hiotellis and Y. S. Hahn, *J. Immunol.*, 2001, **167**, 5264–5272.
68 M. D. Gaca, X. Zhou and R. C. Benyon, *J. Hepatol.*, 2002, **36**, 362–369.

69 K. F. Kok, P. J. Wahab, R. H. Houwen, J. P. Drenth, R. A. de Man, B. van Hoek, J. W. Meijer, F. L. Willekens and R. A. de Vries, *Neth. J. Med.*, 2007, **65**, 160–166.
70 A. Topic, T. Alempijevic, A. S. Milutinovic and N. Kovacevic, *Upsala Journal of Medical Sciences*, 2009, **114**, 228–234.
71 M. Wang, R. E. Long, M. A. Comunale, O. Junaidi, J. Marrero, A. M. Di Bisceglie, T. M. Block and A. S. Mehta, *Cancer Epidemiol., Biomarkers Prev.*, 2009, **18**, 1914–1921.
72 W. L. Zhu, B. L. Fan, D. L. Liu and W. X. Zhu, *Anticancer Res.*, 2009, **29**, 2531–2534.
73 O. Dessouki, Y. Kamiya, H. Nagahama, M. Tanaka, S. Suzu, Y. Sasaki and S. Okada, *Biochem. Biophys. Res. Commun.*, 2010, **393**, 331–337.
74 M. D. Boos, K. Ramirez and B. L. Kee, *Immunol. Res.*, 2008, **40**, 193–207.
75 D. N. Krementsov, J. Weng, M. Lambele, N. H. Roy and M. Thali, *Retrovirology*, 2009, **6**, 64.
76 C. I. Popescu and J. Dubuisson, *Biol. Cell*, 2009, **102**, 63–74.
77 D. A. Sheridan, D. A. Price, M. L. Schmid, G. L. Toms, P. Donaldson, D. Neely and M. F. Bassendine, *Aliment. Pharmacol. Ther.*, 2009, **29**, 1282–1290.
78 S. Li, L. Ye, X. Yu, B. Xu, K. Li, X. Zhu, H. Liu, X. Wu and L. Kong, *Virology*, 2009, **391**, 257–264.
79 A. Dlaskova, L. Hlavata and P. Jezek, *Int. J. Biochem. Cell Biol.*, 2008, **40**, 1792–1805.
80 A. M. Pickrell, H. Fukui and C. T. Moraes, *J. Bioenerg. Biomembr.*, 2009, **41**, 453–456.
81 J. F. Huang, C. Y. Dai, M. L. Yu, S. J. Shin, M. Y. Hsieh, C. F. Huang, L. P. Lee, K. D. Lin, Z. Y. Lin, S. C. Chen, L. Y. Wang, W. Y. Chang and W. L. Chuang, *J. Hepatol.*, 2009, **50**, 471–478.
82 R. De Francesco and G. Migliaccio, *Nature*, 2005, **436**, 953–960.
83 C. L. Murray and C. M. Rice, *Nature*, 2010, **465**, 42–44.
84 N. Kato, K. Mori, K. Abe, H. Dansako, M. Kuroki, Y. Ariumi, T. Wakita and M. Ikeda, *Virus Res.*, 2009, **146**, 41–50.
85 X. Peng, L. E. Cuff, C. D. Lawton and K. A. DeMali, *J. Cell Sci.*, 2010, **123**, 567–577.
86 T. Wakita, T. Pietschmann, T. Kato, T. Date, M. Miyamoto, Z. Zhao, K. Murthy, A. Habermann, H. G. Krausslich, M. Mizokami, R. Bartenschlager and T. J. Liang, *Nat. Med. (N. Y.)*, 2005, **11**, 791–796.
87 Y. Bungyoku, I. Shoji, T. Makine, T. Adachi, K. Hayashida, M. Nagano-Fujii, Y. H. Ide, L. Deng and H. Hotta, *J. Gen. Virol.*, 2009, **90**, 1681–1691.
88 T. Pietschmann, V. Lohmann, A. Kaul, N. Krieger, G. Rinck, G. Rutter, D. Strand and R. Bartenschlager, *J. Virol.*, 2002, **76**, 4008–4021.
89 S. Zeuzem, *Nat. Clin. Pract. Gastroenterol. Hepatol.*, 2008, **5**, 610–622.
90 C. Stark, B. J. Breitkreutz, T. Reguly, L. Boucher, A. Breitkreutz and M. Tyers, *Nucleic Acids Res.*, 2006, **34**, D535–539.
91 C. Yamasaki, K. Murakami, Y. Fujii, Y. Sato, E. Harada, J. Takeda, T. Taniya, R. Sakate, S. Kikugawa, M. Shimada, M. Tanino, K. O. Koyanagi, R. A. Barrero, C. Gough, H. W. Chun, T. Habara, H. Hanaoka, Y. Hayakawa, P. B. Hilton, Y. Kaneko, M. Kanno, Y. Kawahara, T. Kawamura, A. Matsuya, N. Nagata, K. Nishikata, A. O. Noda, S. Nurimoto, N. Saichi, H. Sakai, R. Sanbonmatsu, R. Shiba, M. Suzuki, K. Takabayashi, A. Takahashi, T. Tamura, M. Tanaka, S. Tanaka, F. Todokoro, K. Yamaguchi, N. Yamamoto, T. Okido, J. Mashima, A. Hashizume, L. Jin, K. B. Lee, Y. C. Lin, A. Nozaki, K. Sakai, M. Tada, S. Miyazaki, T. Makino, H. Ohyanagi, N. Osato, N. Tanaka, Y. Suzuki, K. Ikeo, N. Saitou, H. Sugawara, C. O'Donovan, T. Kulikova, E. Whitfield, B. Halligan, M. Shimoyama, S. Twigger, K. Yura, K. Kimura, T. Yasuda, T. Nishikawa, Y. Akiyama, C. Motono, Y. Mukai, H. Nagasaki, M. Suwa, P. Horton, R. Kikuno, O. Ohara, D. Lancet, E. Eveno, E. Graudens, S. Imbeaud, M. A. Debily, Y. Hayashizaki, C. Amid, M. Han, A. Osanger, T. Endo, M. A. Thomas, M. Hirakawa, W. Makalowski, M. Nakao, N. S. Kim, H. S. Yoo, S. J. De Souza, F. Bonaldo Mde, Y. Niimura, V. Kuryshev, I. Schupp, S. Wiemann, M. Bellgard, M. Shionyu, L. Jia, D. Thierry-Mieg, J. Thierry-Mieg, L. Wagner, Q. Zhang, M. Go, S. Minoshima, M. Ohtsubo, K. Hanada, P. Tonellato, T. Isogai, J. Zhang, B. Lenhard, S. Kim, Z. Chen, U. Hinz, A. Estreicher, K. Nakai, I. Makalowska, W. Hide, N. Tiffin, L. Wilming, R. Chakraborty, M. B. Soares, M. L. Chiusano, C. Auffray, Y. Yamaguchi-Kabata, T. Itoh, T. Hishiki, S. Fukuchi, K. Nishikawa, S. Sugano, N. Nomura, Y. Tateno, T. Imanishi and T. Gojobori, *Nucleic Acids Res.*, 2008, **36**, D793–799.
92 M. S. Cline, M. Smoot, E. Cerami, A. Kuchinsky, N. Landys, C. Workman, R. Christmas, I. Avila-Campilo, M. Creech, B. Gross, K. Hanspers, R. Isserlin, R. Kelley, S. Killcoyne, S. Lotia, S. Maere, J. Morris, K. Ono, V. Pavlovic, A. R. Pico, A. Vailaya, P. L. Wang, A. Adler, B. R. Conklin, L. Hood, M. Kuiper, C. Sander, I. Schmulevich, B. Schwikowski, G. J. Warner, T. Ideker and G. D. Bader, *Nat. Protoc.*, 2007, **2**, 2366–2382.
93 Y. Assenov, F. Ramirez, S. E. Schelhorn, T. Lengauer and M. Albrecht, *Bioinformatics*, 2008, **24**, 282–284.
94 Y. Benjamini and Y. Hochberg, *J. R. Stat. Soc. Ser. B*, 1995, **57**, 289–300.
95 W. S. Noble, *Nat. Biotechnol.*, 2009, **27**, 1135–1137.
96 T. Okamoto, H. Omori, Y. Kaname, T. Abe, Y. Nishimura, T. Suzuki, T. Miyamura, T. Yoshimori, K. Moriishi and Y. Matsuura, *J. Virol.*, 2008, **82**, 3480–3489.
97 T. Kato, T. Date, M. Miyamoto, A. Furusaka, K. Tokushige, M. Mizokami and T. Wakita, *Gastroenterology*, 2003, **125**, 1808–1817.

Virus Research 155 (2011) 349–351

Contents lists available at ScienceDirect

Virus Research

journal homepage: www.elsevier.com/locate/virusres

Short communication

Peripheral blood memory B cells are resistant to apoptosis in chronic hepatitis C patients

Toshiaki Mizuochi[a,*], Masahiko Ito[a], Kenji Takai[b], Kazunari Yamaguchi[a]

[a] Department of Research on Blood and Biological Products, 4-7-1 Gakuen, Musashi-Murayama, Tokyo 208-0011, Japan
[b] Cellular Immunology Section, Center for Medical Scientific Analysis, SRL, Inc., 51 Komiyacho, Hachioji-shi, Tokyo 192-8535, Japan

ARTICLE INFO

Article history:
Received 9 July 2010
Received in revised form
21 September 2010
Accepted 21 September 2010
Available online 25 September 2010

Keywords:
HCV
Memory B cell
Apoptosis

ABSTRACT

Our recent study indicated that peripheral B cells in chronic hepatitis C (CHC) patients were infected with hepatitis C virus (HCV). It was also demonstrated that the frequency of $CD27^+$ B cells, i.e. memory phenotype, was significantly reduced in the peripheral blood of CHC patients. An assumption was made by these findings that the $CD27^+$ B cells are susceptible to apoptosis when infected with HCV. Therefore, in this study, the susceptibility of $CD27^+$ B cells to apoptosis in CHC patients was analyzed. Contrary to our assumption, it was found that $CD27^+$ B cells are more resistant to apoptosis than the counterpart subset, i.e. $CD27^-$ B cells. The rationale for this finding is discussed with regard to the possible role for memory B cells as an HCV reservoir for persistent infection in CHC patients.

Hepatitis C virus (HCV) infection has been recognized as one of the major causes of chronic liver diseases, including chronic hepatitis, cirrhosis and, eventually hepatocellular carcinoma, affecting nearly 200 million people worldwide (Lauer and Walker, 2001). The liver is considered to be the primary and main target of HCV infection. However, extrahepatic manifestations, such as mixed cryoglobulinemia, a systemic immune complex-mediated disorder characterized by B cell proliferation that may evolve into overt B cell non-Hodgkin's lymphoma, have been demonstrated (Agnello et al., 1992; Zuckerman et al., 1997). The occurrence of B cell abnormalities often noticed among patients persistently infected with the HCV has suggested the possibility that HCV infects not only hepatocytes but also peripheral B cells. Recent studies including ours have demonstrated that peripheral B cells are in fact infected with HCV (Inokuchi et al., 2009; Ito et al., 2010), which suggest the unprecedented role for B cells in HCV pathogenesis.

Two major human peripheral B cell subsets have been identified based on the expression of CD27, a member of the tumor necrosis factor receptor family. Functional differences between the two subsets have been extensively investigated and it is now generally accepted that CD27 is a memory B cell marker (Agematsu et al., 2000). Our previous study demonstrated that the frequency of peripheral $CD27^+$ memory B cell subset in chronic hepatitis C (CHC) patients is significantly reduced (Mizuochi et al., 2010). To elucidate the reason of this reduction, in this study, we compared the susceptibility of the peripheral $CD27^+$ and $CD27^-$ B cell subsets to apoptosis in CHC patients. Our results demonstrated that $CD27^+$ memory B cells in CHC patients are more resistant to apoptosis than $CD27^-$ B cells. The rationale for this finding is discussed with regard to the possible role for memory B cells in HCV pathogenesis.

A total of 26 CHC patients were enrolled in this study (male/female: 15/11, mean age: 59.6 ± 6.9 years old, mean serum ALT levels: 65.5 ± 31.7 IU/L, mean serum AST levels: 53.2 ± 24.4 IU/L, HCV genotype: 1b = 23, 2a = 3, mean HCV RNA: 2493 ± 959 KIU/mL). All of them were confirmed to be negative for other viral infections, including hepatitis B virus (HBV) and human immunodeficiency virus (HIV). The study protocols were approved by the Review Board at the National Institute of Infectious Diseases. All donors gave written informed consent. The controls were 15 healthy blood donors at the Tokyo Red Cross Blood Center (Tokyo, Japan), who were confirmed to be negative for HCV, HBV, and HIV. HCV genotype was determined by PCR of the core region with genotype-specific primers (Ohno et al., 1997). HCV RNA was quantified by the Roche Amplicor assay (Roche Diagnostics, Branchberg, NJ), and results were standardized to international units (IU). Determination of serum levels of ALT and AST was performed using standard methods.

The following fluorescence-conjugated antibodies (Abs) were used for flow cytometry: Allophycocyanin-anti-CD19 (Cat. MHCD1905; Invitrogen, Carlsbad, CA); PE-anti-CD27 (Cat. IM2578; Beckman Coulter, Fullerton, CA); and FITC-anti-CD27 (Cat. 555440; BD Biosciences, San Jose, CA). Cells were washed twice with cold PBS containing 0.2% BSA, followed by incubation with an appro-

Abbreviations: CHC, chronic hepatitis C patients; HCV, hepatitis C virus.

* Corresponding author. Tel.: +81 42 561 0771; fax: +81 42 562 7875.
E-mail address: miz@nih.go.jp (T. Mizuochi).

0168-1702/$ – see front matter © 2010 Elsevier B.V. All rights reserved.
doi:10.1016/j.virusres.2010.09.017

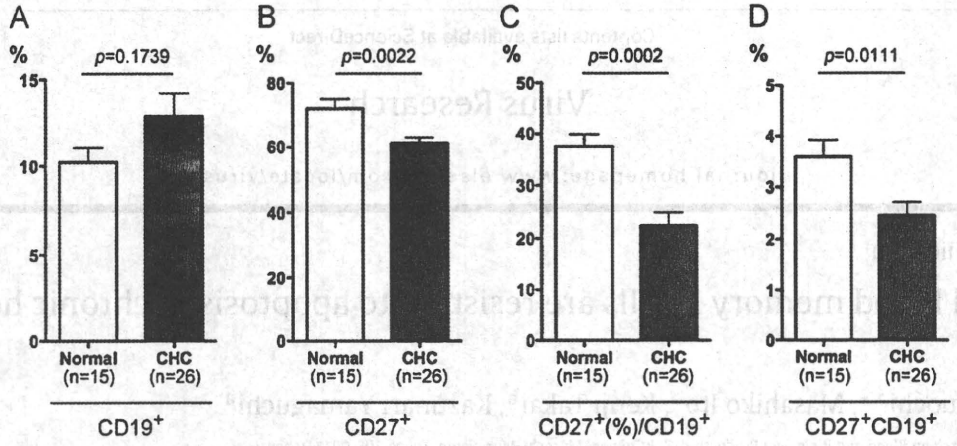

Fig. 1. Flow cytometric analysis of PBMC from normal subjects and CHC patients. Lymphocytes were identified by forward and orthogonal light scatter characteristics. Percentages of $CD19^+$ cells (A), $CD27^+$ cells (B), $CD27^+$ (%) in $CD19^+$ cells (C) and $CD27^+CD19^+$ cells (D) in normal ($n = 15$) and CHC patients ($n = 26$) are shown with SEM bars and p-values.

priate combination of directly conjugated Abs for 30 min on ice. Stained cells were analyzed by FACSCallibur (Becton Dickinson, San Jose, CA). Data were collected using CellQuest software (Becton Dickinson, San Jose, CA) and were analyzed using FlowJo software (Tree Star Inc., Ashland, OR).

Levels of Annexin V binding to both $CD27^+$ and $CD27^-$ B cells were assessed with a commercially available Annexin V apoptosis detection kit Annexin V-FITC (PN IM3546, Beckman Coulter, Fullerton, CA) according to the manufacturer's instructions.

Unpaired (two-tailed) Student's t-test was applied at the 95% confidence level ($p < 0.05$) using Prism ver.4 (GraphPad Software, Inc., San Diego, CA) in all cases.

We first analyzed the frequencies of peripheral blood $CD19^+$ cells, i.e. B cells. They were not statistically different ($p = 0.1739$) between normal subjects and CHC patients as shown in Fig. 1A. When the percentages of peripheral $CD27^+$ cells were analyzed, a statistically significant ($p = 0.0022$) decrease was noticed in CHC patients when compared to normal subjects (Fig. 1B). The percentages of peripheral $CD27^+$ cells in $CD19^+$ cells were then analyzed. A significant ($p = 0.0002$) decrease was noticed in CHC patients when compared to normal subjects (Fig. 1C). It was also verified that the frequencies of peripheral $CD27^+CD19^+$ cells were significantly ($p = 0.01111$) reduced in CHC patients (Fig. 1D). These results are in good agreement with those of Racanelli et al. (2006). In their report, patients with higher plasma HCV loads had lower percentages of $CD27^+$ B cells, thus suggesting that high HCV replication is associated with a reduction in $CD27^+$ B cells. They hypothesized that, under conditions of persisting HCV antigenemia, memory B cells not receiving specific B cell receptor triggering before having T-cell help would be pushed to enhance immunoglobulin production and prone to apoptosis (Racanelli et al., 2006), which may explain the reduction of $CD27^+$ memory B cells in HCV-infected patients. We next examined this possibility by analyzing apoptosis in both peripheral blood $CD27^+$ and $CD27^-$ B cells.

The levels of spontaneous apoptosis among peripheral blood $CD27^+$ and $CD27^-$ B cells in both normal subjects and CHC patients were analyzed using three-color flow cytometry by staining with allophycocyanin-anti-CD19, PE-anti-CD27 and Annexin V-FITC. As shown in Fig. 2A, $CD27^-$ B cells bound to much larger amounts of Annexin V than $CD27^+$ B cells in CHC patients. In contrast, the pat-

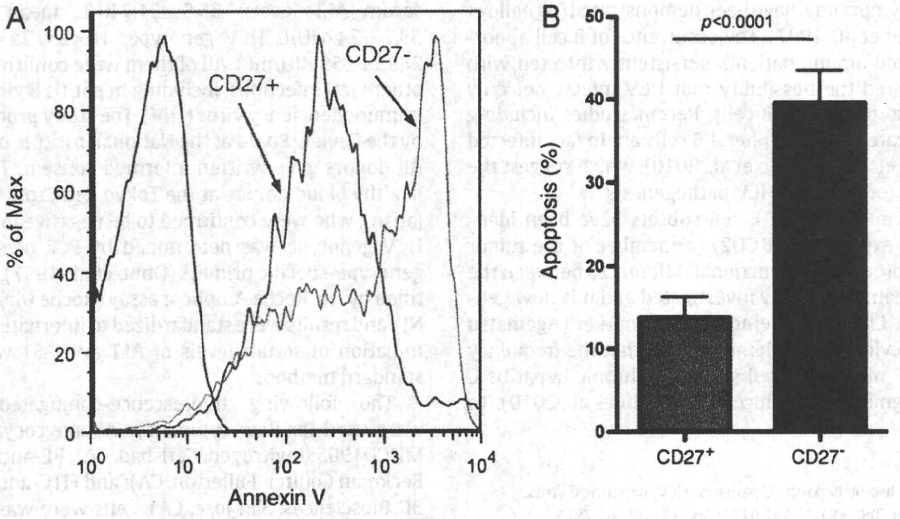

Fig. 2. Annexin V binding to $CD27^+$ and $CD27^-$ B cells. Representative staining patterns for Annexin V binding to $CD27^+$ (red line) and $CD27^-$ (green line) B cells are shown in CHC patients (A). Blue lines indicate background (bkg) staining in negative controls. Summary of data on Annexin V binding to $CD27^+$ (red bar) and $CD27^-$ (green bar) B cells in normal subjects ($n = 8$) and CHC patients ($n = 9$) are shown with SEM bars and p-value (B). (For interpretation of the references to color in this figure legend, the reader is referred to the web version of the article.).

terns of Annexin V binding were similar between $CD27^+$ and $CD27^-$ B cells in normal subjects (data not shown). The percentages of each cell subset bound to large amounts of Annexin V are shown in Fig. 2B (the cut-off point was tentatively set at a fluorescence intensity of 2000). It was concluded that, $CD27^-$ B cells were more vulnerable to apoptosis than $CD27^+$ B cells upon HCV infection; in other words, $CD27^+$ B cells were apparently resistant to apoptosis.

Hepatocytes have long been recognized as main cellular sites for HCV infection. However, this does not necessarily imply that hepatocytes are the exclusive targets for HCV infection. It would be of benefit for HCV to seek other cellular compartments as reservoirs in the event that the liver becomes unsuitable for HCV replication, possibly due to cellular destruction caused by the host immune response. Our recent study verified that peripheral $CD19^+$ B cells in CHC are in fact infected with HCV, thus suggesting a new viral reservoir during the course of natural HCV infection in humans (Ito et al., 2010). Interestingly, another recent study of ours demonstrated that $CD27^+$ B cells are recruited from peripheral blood to the inflammatory site of the liver of CHC patients (Mizuochi et al., 2010). The present study thus may offer new insights into the role of memory B cells in HCV pathogenesis. We assume that memory B cells are the main extrahepatic reservoir of HCV infection because of their long life span which may be correlated with their apparent resistance to apoptosis. This would be a robust strategy for HCV in order to secure sites for persistent infection.

In conclusion, the present study demonstrated that $CD27^+$ B cell subsets in CHC patients are resistant to apoptosis. The long-life of memory $CD27^+$ B cells may be suitable for persistent infection of HCV. Therefore, elimination of peripheral $CD27^+$ B cells in CHC patients with anti-B cell monoclonal antibodies, such as rituximab, would be effective for HCV clearance in CHC patients. Additional study with large sample number and infection with distinct HCV genotype may offer further information.

Acknowledgments

We would like to thank Drs. Miho Suzuki and Kenji Ikebuchi for providing the CHC blood samples used in this study. This study was supported by Grants-in-Aid from the Ministry of Health, Labour, and Welfare.

References

Agematsu, K., Hokibara, S., Nagumo, H., Komiyama, A., 2000. CD27: a memory B-cell marker. Immunol. Today 21 (5), 204–206.

Agnello, V., Chung, R.T., Kaplan, L.M., 1992. A role for hepatitis C virus infection in type II cryoglobulinemia. N. Engl. J. Med. 327 (21), 1490–1495.

Inokuchi, M., Ito, T., Uchikoshi, M., Shimozuma, Y., Morikawa, K., Nozawa, H., Shimazaki, T., Hiroishi, K., Miyakawa, Y., Imawari, M., 2009. Infection of B cells with hepatitis C virus for the development of lymphoproliferative disorders in patients with chronic hepatitis C. J. Med. Virol. 81 (4), 619–627.

Ito, M., Murakami, K., Suzuki, T., Mochida, K., Suzuki, M., Ikebuchi, K., Yamaguchi, K., Mizuochi, T., 2010. Enhanced expression of lymphomagenesis-related genes in peripheral blood B cells of chronic hepatitis C patients. Clin. Immunol. 135 (3), 459–465.

Lauer, G.M., Walker, B.D., 2001. Hepatitis C virus infection. N. Engl. J. Med. 345 (1), 41–52.

Mizuochi, T., Ito, M., Saito, K., Kasai, M., Kunimura, T., Morohoshi, T., Momose, H., Hamaguchi, I., Takai, K., Iino, S., Suzuki, M., Mochida, S., Ikebuchi, K., Yamaguchi, K., 2010. Possible recruitment of peripheral blood CXCR3+ CD27+ CD19+ B cells to the liver of chronic hepatitis C patients. J. Interferon Cytokine Res. 30 (4), 243–252.

Ohno, O., Mizokami, M., Wu, R.R., Saleh, M.G., Ohba, K., Orito, E., Mukaide, M., Williams, R., Lau, J.Y., 1997. New hepatitis C virus (HCV) genotyping system that allows for identification of HCV genotypes 1a, 1b, 2a, 2b, 3a, 3b, 4, 5a, and 6a. J. Clin. Microbiol. 35 (1), 201–207.

Racanelli, V., Frassanito, M.A., Leone, P., Galiano, M., De Re, V., Silvestris, F., Dammacco, F., 2006. Antibody production and in vitro behavior of CD27-defined B-cell subsets: persistent hepatitis C virus infection changes the rules. J. Virol. 80 (8), 3923–3934.

Zuckerman, E., Zuckerman, T., Levine, A.M., Douer, D., Gutekunst, K., Mizokami, M., Qian, D.G., Velankar, M., Nathwani, B.N., Fong, T.L., 1997. Hepatitis C virus infection in patients with B-cell non-Hodgkin lymphoma. Ann. Intern. Med. 127 (6), 423–428.

Research Article

Journal of Innate Immunity

J Innate Immun
DOI: 10.1159/000317690

Received: February 26, 2010
Accepted after revision: June 14, 2010
Published online: August 17, 2010

Peripheral B Cells May Serve as a Reservoir for Persistent Hepatitis C Virus Infection

Masahiko Ito[a] Atsuko Masumi[a] Keiko Mochida[b] Hiroshi Kukihara[c]
Kohji Moriishi[c] Yoshiharu Matsuura[c] Kazunari Yamaguchi[a] Toshiaki Mizuochi[a]

Departments of [a]Research on Blood and Biological Products, and [b]Bacterial Pathogenesis and Infection, National Institute of Infectious Diseases, Tokyo, and [c]Department of Molecular Virology, Research Institute for Microbial Diseases, Osaka University, Suita, Japan

Key Words
Hepatitis C virus · B cells · Retinoic acid-inducible gene-I · Interferon promoter-stimulator-1 · Interferon regulatory factor-3 · Interferon β

Abstract
A recent study by our group indicated that peripheral B cells in chronic hepatitis C (CHC) patients are infected with hepatitis C virus (HCV). This raised the logical question of how HCV circumvents the antiviral immune responses of B cells. Because type I interferon (IFN) plays a critical role in the innate antiviral immune response, IFNβ expression levels in peripheral B cells from CHC patients were analyzed, and these levels were found to be comparable to those in normal B cells, which suggested that HCV infection failed to trigger antiviral immune responses in B cells. Sensing mechanisms for invading viruses in host immune cells involve Toll-like receptor-mediated and retinoic acid-inducible gene-I (RIG-I)-mediated pathways. Both pathways culminate in IFN regulatory factor-3 (IRF-3) translocation into the nucleus for IFNβ gene transcription. Although the expression levels of RIG-I and its adaptor molecule, IFN promoter-stimulator-1, were substantially enhanced in CHC B cells, dimerization and subsequent nuclear translocation of IRF-3 were not detectable. TANK-binding kinase-1 (TBK1) and IκB kinase ε (IKKε) are essential for IRF-3 phosphorylation. Constitutive expression of both kinases was markedly enhanced in CHC B cells. However, reduced expression of heat shock protein of 90 kDa, a TBK1 stabilizer, and enhanced expression of SIKE, an IKKε suppressor, were observed in CHC B cells, which might suppress the kinase activity of TBK1/IKKε for IRF-3 phosphorylation. In addition, the expression of vesicle-associated membrane protein-associated protein-C, a putative inhibitor of HCV replication, was negligible in B cells. These results strongly suggest that HCV utilizes B cells as a reservoir for persistent infection.

Introduction

Hepatitis C virus (HCV) is an enveloped positive-stranded RNA virus that belongs to the *Flaviviridae* family [1]. It is responsible for public health problems worldwide and affects nearly 200 million people [2]. The liver is regarded as the primary target of HCV infection; however, HCV infection is also associated with B cell lymphoproliferative disorders such as mixed cryoglobulinemia and B cell non-Hodgkin lymphoma [3, 4]. In fact, epidemiological evidence suggests a close link between chronic HCV infection and B cell non-Hodgkin lymphoma [5,

KARGER
Fax +41 61 306 12 34
E-Mail karger@karger.ch
www.karger.com

1662–811X/10/0000–0000$26.00/0

Accessible online at:
www.karger.com/jin

Dr. Toshiaki Mizuochi
Department of Research on Blood and Biological Products
National Institute of Infectious Diseases
4-7-1 Gakuen, Musashi-Murayama, Tokyo 208-0011 (Japan)
Tel. +81 42 561 0771, ext. 3243, Fax +81 42 562 7875, E-Mail miz@nih.go.jp

6]. A pathogenic role for HCV in B cell disorders has been further demonstrated by reports showing clinical resolution of the above-mentioned B cell disorders after successful anti-HCV treatment with interferons (IFNs) [3, 7]. Based on this circumstantial evidence, a possible role for B cells in HCV pathogenesis has been postulated, although this has not been conclusively demonstrated.

A body of evidence suggests that HCV RNA replication occurs in a variety of extrahepatic cells, including peripheral dendritic cells, monocytes and macrophages [8–10]. It has also been suggested that HCV preferentially infects B cells that express CD81, a putative HCV receptor molecule [11–14]. A recent study by our group verified that peripheral CD19+ B cells in chronic hepatitis C (CHC) patients were infected with HCV, which suggested a new viral reservoir during the course of natural HCV infection in humans [15]. Thus, we assume that HCV has an escape strategy for persistent infection of B cells.

Foy et al. [16] found that nonstructural (NS) HCV proteins could inhibit the activation of early signaling pathways, such as Toll-like receptor 3 (TLR3)- and retinoic acid-inducible gene-I (RIG-I)-mediated pathways, which lead to IFNβ production. These results indicated that HCV NS3/4A serine protease blocked IFN regulatory factor-3 (IRF-3) activation upon HCV infection in the human hepatoma cell line HuH-7. Subsequent studies have shown that NS3/4A blocks IFN promoter-stimulator-1 (IPS-1)-mediated signaling pathways by cleaving the IPS-1 molecule and impeding downstream IRF-3 activation [17]. Thus, HCV apparently has a strategy to evade host innate immunity. However, recent studies by Dansako et al. [18, 19] found that the effects of HCV NS3/4A protease on IFN production depended on the cell lines used, because a non-neoplastic human hepatocyte cell line, PH5CH8 [20], retained both TLR3- and RIG-I-mediated pathways, in contrast to HuH-7 cells, which lack the former pathway [21]. However, no studies have examined the effects of HCV infection on IFN responses of nonhepatic cell lines.

In this study, we aimed to understand the mechanisms by which HCV evades innate immune responses in CHC B cells. We found that the antiviral immune response, represented by IFNβ induction, was severely impaired in B cells of CHC patients. Our results strongly suggest that the IRF-3 activation cascade is impeded in B cells upon HCV infection. Thus, IFNβ gene transcription is not augmented, which may result in failed IFNβ-inducible antiviral responses in CHC B cells. Furthermore, the expression of vesicle-associated membrane protein-associated protein-C (VAP-C), a putative inhibitor of HCV replication, was negligible in B cells. These results support the notion that HCV can successfully reside in B cells, resulting in persistent infection. This is the first study describing analysis of the suppressive effects of HCV infection on antiviral innate immunity in peripheral B cells. Thus, this study offers new insights into the role of B cells in the pathogenesis of HCV.

Methods

Patients and Samples

A total of 24 CHC patients were enrolled in this study, with the following characteristics: 14 males and 10 females; mean age 62.4 ± 7.4 years; mean serum ALT levels 67.5 ± 36.0 IU/l; mean serum AST levels 66.7 ± 34.3 IU/l; 21 patients with HCV genotype 1b and 3 with HCV genotype 2a, and mean HCV RNA 1,752 ± 1,188 KIU/ml. All cases were confirmed to be negative for other viral infections, including hepatitis B virus and human immunodeficiency virus. The study protocols were approved by the Review Board of the National Institute of Infectious Diseases. All donors gave written informed consent. Controls were healthy blood donors at the Tokyo Red Cross Blood Center (Tokyo, Japan) who were confirmed to be negative for HCV, hepatitis B virus and human immunodeficiency virus.

Peripheral blood mononuclear cells (PBMCs) were isolated by Ficoll-Hypaque (Pharmacia Biotech, Quebec, Que., Canada) density gradient centrifugation. CD19+ B lymphocytes were isolated from PBMCs by negative selection (B Cell Isolation Kit II, human; Miltenyi, Auburn, Calif., USA). The purity of isolated B cells was generally >95%, as assessed by flow cytometry.

Semiquantitative Real-Time PCR

Total RNA was extracted from lymphoid cells using Isogen (Nippon Gene Co. Ltd., Tokyo, Japan). cDNA was synthesized using SuperScript III Reverse Transcriptase (Invitrogen, Carlsbad, Calif., USA) with oligo(dT)12–18 primer (Invitrogen). PCR amplification was performed using SYBR Premix Ex Taq™ II (Takara Shuzo, Kyoto, Japan) with gene-specific primers (Bex Co. Ltd., Tokyo, Japan) available in the public database RTPrimerDB [22] under the codes 3542 for IFNβ and 3539 for GAPDH, and the Universal Probe Library Assay Design Center (https://www.roche-applied-science.com/sis/rtpcr/upl/index.jsp; Roche Applied Science) as follows: IPS-1 (No. 19, 04686926001), TIR domain-containing adaptor inducing IFN (TRIF; No. 37, 04687957001), suppressor of IκB kinase ε (IKKε) (SIKE; No. 56, 04688538001), heat-shock protein of 90 kDa (Hsp90; No. 25, 04686993001) and DEAD (Asp-Glu-Ala-Asp) box polypeptide 3, X-linked (DDX3X; No. 69, 04688686001). The primer sequences for RIG-I were 5′-GTG CAA AGC CTT GGC ATG T-3′ (forward) and 5′-TGG CTT GGG ATG TGG TCT ACT C-3′ (reverse) [23], and for TLR3 they were 5′-GTT ACG AAG AGG CTG GAA TGG T-3′ (forward) and 5′-GCC AGG AAT GGA GAG GTC TAG A-3′ (reverse) [24].

Real-time PCR was carried out for 45 cycles at 94°C for 1 min and at 60°C for 25 s (two-step PCR) using a Light Cycler (Roche Diagnostics, Basel, Switzerland). Amplification of predicted fragments was confirmed by melt curve analysis and gel electropho-

resis. Standard curves were established with 10-fold serial dilutions of amplified products. Measured amounts of each mRNA were normalized to GAPDH mRNA. mRNA expression levels in normal B cells were arbitrarily defined as 1.0.

Immunoblot Analysis

To extract whole-cell proteins, cell pellets were suspended in modified RIPA buffer [150 mM NaCl, 50 mM Tris-Cl (pH 7.4), 1 mM EDTA, 1.0% NP-40, 0.5% sodium deoxycholic acid and 0.1% SDS] containing Halt protease inhibitor cocktail (Pierce, Rockford, Ill., USA) and Halt phosphatase inhibitor cocktail (Pierce; 2×10^7 cells/ml). After 20 min of incubation on ice, cell extracts were centrifuged at 12,000 *g* for 10 min at 4°C, transferred to other tubes and stored at –80°C. Nuclear and cytoplasmic proteins were separated using a Nuclear Extraction Kit (Active Motif, Carlsbad, Calif., USA) according to the manufacturer's protocol. Protein concentration was determined using the BCA™ Protein Assay Kit – Reducing Agent Compatible (Pierce). Samples (whole-cell extract, 1 g; fractionated extract, 2×10^5 cells) were loaded onto 7.5 or 12.5% SDS acrylamide gels (Real Gel Plate; Bio Craft, Tokyo, Japan), followed by transfer to polyvinylidene difluoride membranes. Membranes were blocked for 1 h at room temperature using Block Ace™ (Dainippon Sumitomo Pharma Co. Ltd., Osaka, Japan). They were then sequentially probed with primary and secondary antibodies at 4°C overnight and for 1 h at room temperature, respectively.

For primary antibodies, we used anti-IFN rabbit polyclonal antibody (ab9662, 1/1,000 dilution; Abcam Inc., Cambridge, Mass., USA), anti-ACTB (β-actin) rabbit polyclonal antibody (4967, 1/1,000 dilution; Cell Signaling Technology, Danvers, Mass., USA), anti-TLR3 rabbit polyclonal antibody (ab62566, 1/1,000 dilution; Abcam), anti-TRIF rabbit polyclonal antibody (4596, 1/1,000 dilution; Cell Signaling Technology), anti-RIG-I rabbit polyclonal antibody (29010, 1/100 dilution; Immuno-Biological Laboratories Co. Ltd., Gunma, Japan), anti-IPS-1 rabbit polyclonal antibody (AT107, 1/2,000 dilution; Alexis Biochemicals, Farmingdale, N.Y., USA), anti-IRF-3 rabbit polyclonal antibody (18781, 1/100 dilution; Immuno-Biological Laboratories), anti-GAPDH mouse monoclonal antibody [5G4(6C5), 1/9,000 dilution; HyTest Ltd., Turku, Finland], anti-PARP-1 mouse monoclonal antibody (AM30, 1/500 dilution; Calbiochem, San Diego, Calif., USA), anti-TANK-binding kinase-1 (TBK1) rabbit polyclonal antibody (3504, 1/1,000 dilution; Cell Signaling Technology) and anti-IKKε rabbit polyclonal antibody (ab7891, 1/500 dilution; Abcam). Anti-VAP-C rabbit polyclonal antibody (2.66 g/ml) was produced by a group of the authors (H.K., K. Moriishi and Y.M.).

The secondary antibodies used were horseradish peroxidase-coupled donkey anti-rabbit Ig (NA934, 1/10,000 dilution; GE Healthcare Ltd.; UK, Buckinghamshire, UK) and horseradish peroxidase-coupled sheep anti-mouse Ig (NA931, 1/10,000 dilution; GE Healthcare UK). Protein bands were detected using ECL Plus™ Western Blotting Detection Reagents (GE Healthcare UK) and a LAS-3000 Image Analyzer (Fuji Film, Tokyo, Japan). Densitometric analysis was performed within a linear range using Image Gauge (Fuji Film). The density of each band (the amount of protein) was normalized against that of the corresponding β-actin.

Native PAGE for IRF-3 Dimer Detection

Native PAGE was performed using 7.5% SDS acrylamide gels (Real Gel Plate; Bio Craft). Gels were prerun with 25 mM Tris-Cl (pH 8.4) and 192 mM glycine with and without 0.2% deoxycholate in the cathode and anode chambers, respectively, for 30 min at 40 mA. Samples were extracted in lysis buffer (3×10^7 cells/ml; 50 mM Tris-Cl, pH 8.0, 1% NP40, 150 mM NaCl) containing Halt protease inhibitor cocktail and Halt phosphatase inhibitor cocktail, mixed with equal volumes of Tris-glycine native sample buffer (2×; Invitrogen), applied to the gel and electrophoresed for 60 min at 25 mA.

Immunoblotting was performed as described above. As a positive control for IRF-3 dimerization, HeLa cells were added with 100 g/ml polyriboinosinic-polyribocytidylic acid (poly I:C; kindly provided by Toray Co. Ltd., Tokyo, Japan). Three hours after incubation, cells were harvested and cell lysates were prepared as described above.

Poly I:C Transfection

CD19+ B lymphocytes isolated from PBMCs were cultured in RPMI-1640 medium containing 10% FCS, 2 mM L-glutamine, 1 mM HEPES, 0.05 mM β-mercaptoethanol, penicillin and streptomycin in a flat-bottom 96-well plate for 3 h (2.5×10^6 cells/well). To activate the RIG-I-mediated pathway, cells were transfected with 10 μg/ml poly I:C using Poly(I:C)/LyoVec (Invivogen, San Diego, Calif., USA). After 18 h of culture, transfected or non-transfected cells were dissolved in Isogen (Nippon Gene) for semi-quantitative real-time PCR assay. Three independent triplicate transfection experiments were performed in order to verify the reproducibility of the results.

Statistics

Unpaired (two-tailed) Student's t tests were applied at the 95% confidence level ($p < 0.05$) using Prism (version 4; GraphPad Software Inc., San Diego, Calif., USA) in all cases.

Results

Impaired IFN Responses in Peripheral B Cells of CHC Patients

We recently demonstrated that HCV infected and may have replicated in peripheral B cells of CHC patients [15]. This implied that HCV may have evaded the immune response by B cells, resulting in persistent infection. Because the induction of type I IFNs, including IFNβ, is crucial for host defense against invading viruses, we first examined constitutive IFNβ expression levels in peripheral B cells of CHC patients. As shown in figure 1a, IFNβ mRNA expression levels were not augmented in CHC B cells compared with normal B cells. The results of Western blotting analysis (fig. 1b) indicated that constitutive IFNβ protein expression levels were not enhanced in B cells of CHC patients, which supported the finding of unaltered IFNβ mRNA expression.

We then stimulated normal and CHC B cells using poly I:C transfection, which triggers RIG-I- and melanoma differentiation-associated gene-5-mediated IFNβ path-

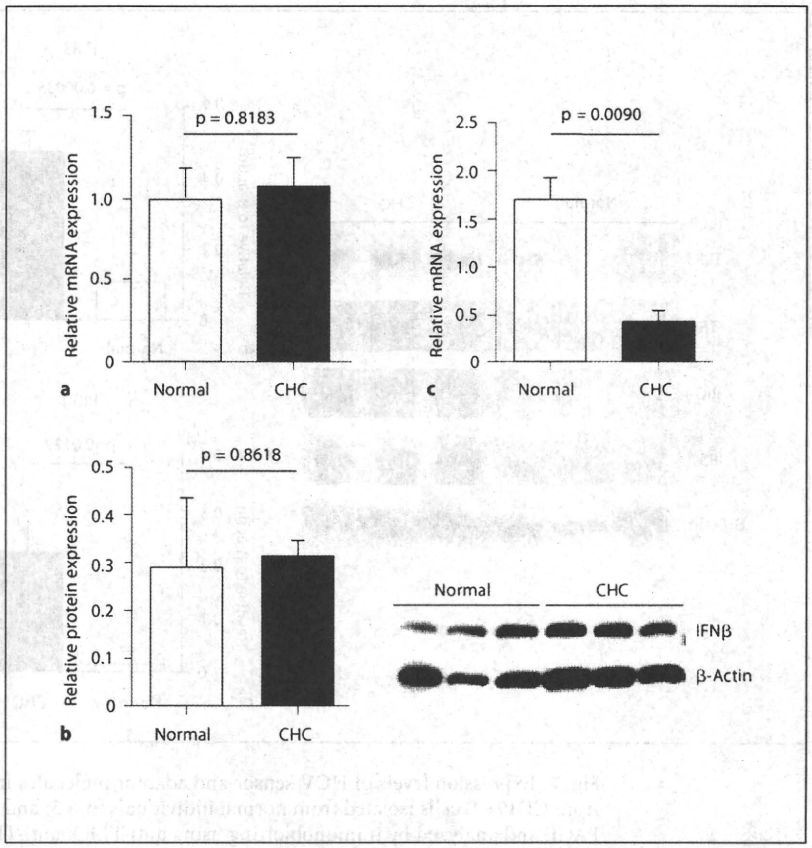

Fig. 1. IFNβ expression in CHC B cells. Fractionation of CD19+ B cells from PBMCs was performed as described in Methods. **a** IFNβ mRNA expression levels in CD19+ B cells isolated from normal individuals (n = 4) and CHC patients (n = 7) were measured in duplicate by quantitative real-time RT-PCR and normalized against those of the housekeeping gene GAPDH. mRNA expression levels in normal B cells were arbitrarily defined as 1.0. **b** Whole-cell extracts prepared from CD19+ B cells isolated from normal individuals (n = 3) and CHC patients (n = 3) were subjected to SDS-PAGE and analyzed by immunoblotting using anti-IFNβ and anti-ACTB antibodies. Relative IFNβ protein expression levels normalized against β-actin expression are shown. **c** CD19+ B cells isolated from normal individuals (n = 3) or CHC patients (n = 3) were transfected with poly I:C (10 g/ml). Eighteen hours after transfection, cells were harvested and total RNA was isolated. IFNβ mRNA expression levels were measured in duplicate using quantitative real-time RT-PCR and normalized against those of the housekeeping gene GAPDH. mRNA expression levels in untransfected normal or CHC B cells were arbitrarily defined as 1.0. Representative results from at least 2 independent experiments with similar results are shown.

ways. As shown in figure 1c, IFNβ mRNA expression levels in CHC B cells were much lower than those in normal B cells, suggesting that CHC B cells are defective with regard to IFNβ production upon stimulation with the intracellular delivery of poly I:C. In addition, the expression levels of IFN-stimulated genes, such as ISG-15 and ISG-56, in CHC B cells were also much lower than those in normal B cells upon poly I:C stimulation (data not shown).

Taken together, these results indicate that chronic HCV infection fails to induce an IFNβ response in CHC B cells. Subsequent experiments were designed to elucidate the underlying mechanism(s) by which HCV interrupted the IFN responses in CHC B cells.

Expression Levels of HCV Sensor Molecules in Peripheral B Cells of CHC Patients

We next examined the gene expression levels in peripheral B cells of two major viral sensors, TLR3 and RIG-I, as well as their corresponding adaptor molecules, TRIF and IPS-1, which are indispensable for initiating innate immune responses [25]. As shown in figure 2, TLR3, TRIF, RIG-I and IPS-1 expression levels were significantly enhanced in peripheral B cells of CHC patients. Expression of another cytoplasmic sensor molecule, melanoma differentiation-associated gene-5, was also enhanced (data not shown). These results demonstrate that the expression levels of cytoplasmic virus sensors as well as their adaptors are constitutively augmented in CHC B cells.

Expression, Dimerization and Nuclear Translocation of IRF-3 in CHC B Cells

The IRF-3 activation cascade, including phosphorylation, dimerization and nuclear translocation, is essential for IFNβ gene transcription [26]. We found that constitutive IRF-3 expression levels in CHC B cells were significantly lower than those in normal B cells (p = 0.0018) as assessed by Western blotting (fig. 3a). Furthermore, IRF-